

OPTIMAL EXPERIMENTAL DESIGN FOR INVERSE PROBLEMS IN THE PRESENCE OF OBSERVATION CORRELATIONS*

AHMED ATTIA[†] AND EMIL CONSTANTINESCU^{†‡}

Abstract. Optimal experimental design (OED) is the general formalism of sensor placement and decisions about the data collection strategy for engineered or natural experiments. This approach is prevalent in many critical fields such as battery design, numerical weather prediction, geosciences, and environmental and urban studies. State-of-the-art computational methods for experimental design, however, do not accommodate correlation structure in observational errors produced by many expensive-to-operate devices such as X-ray machines or radar and satellite retrievals. Discarding evident data correlations leads to biased results, poor data collection decisions, and waste of valuable resources. We present a general formulation of the OED formalism for model-constrained large-scale Bayesian linear inverse problems, where measurement errors are generally correlated. The proposed approach utilizes the Hadamard product of matrices to formulate the weighted likelihood and is valid for both finite- and infinite-dimensional Bayesian inverse problems. We also discuss widely used approaches for relaxation of the binary OED problem, in light of the proposed pointwise weighting approach, and present a clear interpretation of the relaxed design and its effect on the observational error covariance. Extensive numerical experiments are carried out for empirical verification of the proposed approach by using an advection-diffusion model, where the objective is to optimally place a small set of sensors, under a limited budget, to predict the concentration of a contaminant in a bounded domain.

Key words. Optimal experimental design (OED), Inverse problems, Correlated observations, Data assimilation

AMS subject classifications. 62K05, 35Q62, 62F15, 35R30, 35Q93, 65C60

1. Introduction. Sensor placement is the problem of determining the optimal positions of a given number of sensors from a set of candidate locations. This problem is widely formulated as an optimal experimental design (OED) problem [42, 20, 38, 47], where the design determines whether to activate a sensor or not. Bayesian OED for data acquisition and sensor placement has been addressed in the context of ill-posed linear inverse problems [23, 25] and nonlinear inverse problems [24, 29] and has also been considered in infinite-dimensional settings [13, 2, 5, 4, 3, 1]. In our work and the works cited above, linearity is associated with the parameter-to-observable map, which describes the relation between the quantity of interest (QoI) and the observational data.

Scalable data assimilation and uncertainty quantification methodologies have gained significant interest, especially when applied to large- to extreme-scale models, such as the atmosphere and power grid simulations [12, 18, 36, 10, 9]. The underlying principle of these methods is that information collected from observational systems is fused into computational models to produce accurate forecasts of a QoI. This QoI could, for example, refer to the model parameters, initial condition, or the model state. In Bayesian inversion, the goal is to infer the value of the QoI through the posterior distribution of that QoI modeled as a random variable, conditioned by the noisy observational data. The quality of such assimilation systems depends heavily on the extent to which the mathematical assumptions

*Submitted to the editors June 28, 2022.

Funding: This work was partially supported by the U.S. Department of Energy, Office of Science, Advanced Scientific Computing Research Program under contract DE-AC02-06CH11357 and Laboratory Directed Research and Development (LDRD) funding from Argonne National Laboratory.

[†]Mathematics and Computer Science Division, Argonne National Laboratory, Lemont, IL (attia@mcs.anl.gov and emconsta@mcs.anl.gov).

[‡]The University of Chicago, IL.

reflect reality, as well as on the quality of the collected measurements, which in turn depends on the data acquisition schedule and the sensor placement strategy.

An optimal design improves the quality of the observational grid and the collected data and hence improves the model-based forecast made by an assimilation system. Deploying and operating observational instruments can be expensive, however, thus mandating the development of optimal sensor placement strategies and optimal data acquisition schedules. An optimal design is generally found by solving a binary optimization problem, or a relaxation thereof, with the objective of minimizing the uncertainty of the posterior QoI under the constraints forced by the computational model. The objective function of such an optimization problem is formulated based on the choice of the optimality criterion, which is a scalar summary of the uncertainty of the Bayesian inversion QoI. For example, an A-optimal design minimizes the average variance, and a D-optimal design minimizes the generalized variance, which is equivalent to maximizing the differential Shannon information content of the inversion QoI [42].

The presence of observation spatiotemporal error correlations in OED for inverse problems poses a significant challenge [48]. A common approach, which is followed for simplicity in solving model-constrained OED problems, is to drop spatiotemporal correlations and assume that observation errors are temporally and spatially uncorrelated. This approach can be restrictive, however, and is even violated in many applications where a single instrument is used to collect measurements at various orientations, such as X-ray machines, satellites, and light detection and ranging radars.

The statistics literature provides a wealth of treatments of correlated observations in several OED scenarios and settings [17, 34, 35, 40, 16]. For example, the ordinary least-squares approach for inversion and the D-optimality criterion is adopted in [48] to avoid inaccuracies or lack of knowledge of the observation correlation structure. Additionally, OED for correlated observations has been considered in the context of linear regression models, for example in [19, 49]. Nevertheless, in the context of Bayesian inverse problems, more work is needed to provide simple algorithmic OEDs that are suitable for multiple choices of the optimality criterion and are capable of properly handling correlations in observational errors.

In this work we present a generalized OED formulation based on the Hadamard product of the observation error covariance matrix with a symmetric weighting kernel, where the observation errors are generally correlated. In this case the covariances of the observation errors, manifested in the weighted data likelihood, could form a diagonal, a block diagonal, or even a full space-time covariance matrix. This approach provides a generalized formulation of the OED optimality criterion and the associated gradients, where it takes into account the correlation structure of observational errors. Moreover, it enables controlling the influence of observational correlations on the experimental design, for example, by ignoring the effect of spurious correlations, using a space-time weighting kernel. In this paper we extensively analyze the effect of the binary design and the relaxation on the observational error variances/covariances and on the OED objective function. We also discuss the limitation and potential inaccuracy of existing weighting approaches, which have been used in the case of uncorrelated observational errors. The new formulation resolves a common misunderstanding about the effect of the relaxation on the OED optimization objective and on the corresponding optimal design. Moreover, this formulation adds a layer of flexibility to the standard OED formulation in the context of Bayesian inversion and is suitable for both finite- and infinite-dimensional Bayesian linear inversion frameworks. Additionally, the presented approach enables converting the OED constrained optimization problem into an unconstrained optimization problem, which enables utilizing a plethora of efficient numerical optimization routines.

The rest of the paper is structured as follows. [Section 2](#) provides the mathematical background and describes the standard formulation of optimal design of experiments for Bayesian linear inverse problems. The proposed approach for handling errors in observation correlations is described in [Section 3](#), with detailed derivation of formulae given in the appendices included in the supplementary material. The setup and results of numerical experiments are given in [Section 4](#). Concluding remarks are presented in [Section 5](#).

2. Background. Here we review the elements of Bayesian inversion and OED for Bayesian inverse problems governed by computational models, such as partial differential equations (PDEs).

2.1. Bayesian inverse problem. A forward problem describes the relationship between model parameters and observational data. The vast majority of large-scale simulation models follow the forward model described by $\mathbf{y} = \mathcal{F}(\theta) + \delta$, where $\theta \in \mathbb{R}^{N_{\text{state}}}$ is the model parameter and $\mathbf{y} \in \mathbb{R}^{N_{\text{obs}}}$ is the observational data. The forward map \mathcal{F} is a discretized parameter-to-observable operator that maps a model parameter into the observation space, and $\delta \in \mathbb{R}^{N_{\text{obs}}}$ accounts for measurement noise. We restrict the discussion in this work to the case of linear models, that is, $\mathcal{F}(\theta) = \mathbf{F}\theta$:

$$(2.1) \quad \mathbf{y} = \mathbf{F}\theta + \delta.$$

The parameter θ is generally modeled as a random variable with a Gaussian prior $\mathcal{N}(\theta_{\text{pr}}, \mathbf{\Gamma}_{\text{pr}})$. In the Gaussian framework, the observational noise is assumed to be Gaussian, that is, $\delta \sim \mathcal{N}(\mathbf{0}, \mathbf{\Gamma}_{\text{noise}})$, where $\mathbf{\Gamma}_{\text{noise}}$ is the observation error covariance matrix. In this case, the data likelihood is

$$(2.2) \quad \mathcal{L}(\mathbf{y}|\theta) \propto \exp\left(-\frac{1}{2}\|\mathbf{F}\theta - \mathbf{y}\|_{\mathbf{\Gamma}_{\text{noise}}^{-1}}^2\right),$$

where the weighted norm is defined as $\|\mathbf{x}\|_{\mathbf{A}}^2 = \mathbf{x}^T \mathbf{A} \mathbf{x}$.

The inverse problem involves retrieving the underlying model parameter θ from noisy measurements \mathbf{y} , given the specification of prior and observation noise uncertainties. Specifically, in Bayesian inversion we seek the posterior distribution of θ conditioned by observational data \mathbf{y} . For a linear forward operator \mathbf{F} , the posterior is Gaussian $\mathcal{N}(\theta_{\text{post}}^{\mathbf{y}}, \mathbf{\Gamma}_{\text{post}})$ with

$$(2.3) \quad \theta_{\text{post}}^{\mathbf{y}} = \mathbf{\Gamma}_{\text{post}} (\mathbf{\Gamma}_{\text{pr}}^{-1} \theta_{\text{pr}} + \mathbf{F}^* \mathbf{\Gamma}_{\text{noise}}^{-1} \mathbf{y}), \quad \mathbf{\Gamma}_{\text{post}} = (\mathbf{F}^* \mathbf{\Gamma}_{\text{noise}}^{-1} \mathbf{F} + \mathbf{\Gamma}_{\text{pr}}^{-1})^{-1} = \mathbf{H}^{-1},$$

where \mathbf{F}^* is the adjoint of the forward operator \mathbf{F} . Here the posterior mean $\theta_{\text{post}}^{\mathbf{y}}$ provides a posterior estimate of the true value of the parameter θ_{true} , given the prior mean θ_{pr} , the data \mathbf{y} , and the associated uncertainties.

We note that the Hessian \mathbf{H} of the negative log of the posterior probability density function (PDF) is equal to the posterior precision matrix $\mathbf{\Gamma}_{\text{post}}^{-1}$ and is independent from the data. Thus, in the linear Gaussian case one can completely describe the posterior covariances, given the forward operator and both prior and observation noise covariances. Unlike the linear case, however, if the forward operator \mathcal{F} is nonlinear, the posterior covariance depends on the observational data, and the OED problem becomes more difficult and is beyond the scope of this work.

2.2. Goal-oriented Bayesian inverse problem. Solving an inverse problem is often an intermediate step, where the inversion parameter, such as the inferred model parameter, is then used to make further prediction of a goal QoI. We consider the QoI of the form $\gamma = \mathbf{P}\theta \in \mathbb{R}^{N_{\text{goal}}}$, where

\mathbf{P} is a linear *goal operator* [6]. A simple example of \mathbf{P} is an integral operator that evaluates the expected value of the inferred parameter. We follow this general formulation hereafter since the standard Bayesian inverse problem is a special case, where \mathbf{P} is set to the identity operator \mathcal{I} . Given the distribution of the model parameter, the prior of γ is Gaussian $\mathcal{N}(\gamma_{\text{pr}}, \mathbf{\Sigma}_{\text{pr}})$, with $\gamma_{\text{pr}} = \mathbf{P}\theta_{\text{pr}}$, and $\mathbf{\Sigma}_{\text{pr}} = \mathbf{P}\mathbf{\Gamma}_{\text{pr}}\mathbf{P}^*$. The posterior of γ is also Gaussian $\mathcal{N}(\gamma_{\text{post}}, \mathbf{\Sigma}_{\text{post}})$, with

$$(2.4) \quad \gamma_{\text{post}} = \mathbf{P}\mathbf{\Gamma}_{\text{post}} \left(\mathbf{\Gamma}_{\text{pr}}^{-1}\theta_{\text{pr}} + \mathbf{F}^*\mathbf{\Gamma}_{\text{noise}}^{-1}\mathbf{y} \right), \quad \mathbf{\Sigma}_{\text{post}} = \mathbf{P} \left(\mathbf{F}^*\mathbf{\Gamma}_{\text{noise}}^{-1}\mathbf{F} + \mathbf{\Gamma}_{\text{pr}}^{-1} \right)^{-1} \mathbf{P}^*.$$

The exact form of the adjoint of the forward operator \mathbf{F}^* and that of the adjoint of the goal operator \mathbf{P}^* depend on the problem at hand. Specific instances will be discussed in [Section 4](#) in the context of numerical experiments.

2.3. Bayesian OED. In Bayesian OED, we seek a design for the data acquisition process. The specific definition of an experimental design, in general, is problem dependent. For example, an experimental design $\zeta \in \Xi$ can be associated with the configuration of an observational grid; that is, the experimental design describes the sensor placement strategy. In this case an experimental design is said to be optimal if it minimizes the posterior uncertainty of the solution of an inverse problem in some sense. The optimal design ζ^{opt} in the context of an inverse problem is defined by an *optimality criterion*, which in general is a scalar functional $\Psi(\cdot)$ that depends on the posterior uncertainty of the inversion QoI. In the linear Gaussian settings, the optimality criterion is generally set as a scalar summary of the posterior covariance matrix. The traditional alphabetic criteria including A- and D-optimality are the most popular choices [1]. An A-optimal design $\zeta^{\text{A-opt}}$ minimizes the trace of the posterior covariance, while a D-optimal design $\zeta^{\text{D-opt}}$ minimizes its determinant (or equivalently the log-determinant):

$$(2.5) \quad \zeta^{\text{A-opt}} = \arg \min_{\zeta \in \Xi} \Psi^{\text{GA}}(\zeta) := \text{Tr}(\mathbf{\Sigma}_{\text{post}}(\zeta)); \quad \zeta^{\text{D-opt}} = \arg \min_{\zeta \in \Xi} \Psi^{\text{GD}}(\zeta) := \log \det(\mathbf{\Sigma}_{\text{post}}(\zeta)).$$

These optimality criteria are typically augmented by regularization and sparsification terms that are discussed in later sections. Note that the optimization problems (2.5) can be rewritten as maximization by replacing the posterior covariance with the Fisher information matrix.

2.4. Bayesian OED for sensor placement. In the sensor placement problems we seek the *optimal* subset of sensors of size λ from n_s candidate locations. In this case the design $\zeta = \zeta^{\text{b}}$ is a vector of binary entries, whose components can be interpreted as sensors being *active* or *inactive*; that is, $\zeta^{\text{b}} \in \Xi := \{0, 1\}^{n_s}$. When a sensor is deactivated, the row/column in the observation error covariance matrix corresponding to that observation is eliminated from the formulation of the Bayesian inverse problem and is kept when the sensor is active. This can be formulated as a binary optimization problem over the binary design space. Solving a binary OED problem for sensor placement, however, is computationally infeasible for large-scale problems. In practice, the design weights, that is, the integrality of entries $\zeta_i; i = 1, 2, \dots, n_s$, are *relaxed* to take values in the interval $[0, 1]$; that is, $\zeta \in \Xi := [0, 1]^{n_s}$. Then a sparsification is enforced by adding a suitable regularization term to the optimality objective (2.5).

The design enters the inverse problem formulation through the data likelihood as a set of observation weights. Specifically, the observation covariance $\mathbf{\Gamma}_{\text{noise}}$ is replaced with a weighted version $\mathbf{W}_{\Gamma}(\zeta)$, resulting in the weighted data likelihood

$$(2.6) \quad \mathcal{L}(\mathbf{y}|\theta; \zeta) \propto \exp \left(-\frac{1}{2} \|\mathbf{F}\theta - \mathbf{y}\|_{\mathbf{W}_{\Gamma}(\zeta)}^2 \right).$$

The weighted posterior covariance of the inferred QoI in this case is

$$(2.7) \quad \Sigma_{\text{post}}(\zeta) = \mathbf{P}\mathbf{H}^{-1}(\zeta)\mathbf{P}^* = \mathbf{P}(\mathbf{F}^*\mathbf{W}_{\Gamma}(\zeta)\mathbf{F} + \Gamma_{\text{pr}}^{-1})^{-1}\mathbf{P}^*.$$

A common approach to define the weighted inverse covariance matrix $\mathbf{W}_{\Gamma}(\zeta)$, in the case of uncorrelated observation errors, is to introduce a weighting matrix $\mathbf{W}(\zeta)$ and use the form $\mathbf{W}_{\Gamma}(\zeta) := \mathbf{W}^{\frac{1}{2}}(\zeta)\Gamma_{\text{noise}}^{-1}\mathbf{W}^{\frac{1}{2}}(\zeta)$. The design matrix $\mathbf{W} \in \mathbb{R}^{N_{\text{obs}} \times N_{\text{obs}}}$ is a symmetric weighting matrix parameterized by the design ζ . In sensor placement problems, the design is a vector containing weights assigned to each candidate sensor location $\zeta = (\zeta_1, \zeta_2, \dots, \zeta_{n_s})^{\top}$, and the weighting matrix is a diagonal matrix with design weights on the diagonal; that is, $\mathbf{W} = \text{Diag}(\zeta)$. An alternative approach is to use the form $\mathbf{W}_{\Gamma} := \Gamma_{\text{noise}}^{-\frac{1}{2}}\mathbf{W}\Gamma_{\text{noise}}^{-\frac{1}{2}}$. Little attention is given in the literature to the difference between these two forms, mainly because in many applications the observations are assumed to be uncorrelated, resulting in a diagonal covariance matrix Γ_{noise} . In this case these two forms are equivalent. In general, however, they are not. The latter form simplifies the derivation of the gradient of the optimality criterion with respect to the design; however, the interpretability of its effect is not intuitive. On the other hand, the former form weighs the sensor observations, based on their contributed information gain, resulting in a reduction in the QoI posterior uncertainty. Further discussion of the validity of these forms of the weighted precision matrix $\mathbf{W}_{\Gamma}(\zeta)$ is in [Subsection 3.1](#).

In time-dependent settings, the dynamical model is simulated over a window containing observation time instances t_1, t_2, \dots, t_{n_t} . For simplicity we assume the matrix representation of the forward map \mathbf{F} has rows that form consecutive blocks, each corresponding to all spatial measurements at one time moment. Assuming that the design weights associated with candidate observational gridpoints are fixed over time, the weighting matrix $\mathbf{W} \in \mathbb{R}^{N_{\text{obs}} \times N_{\text{obs}}}$ can be defined as $\mathbf{W} = \mathbf{I}_{n_t} \otimes \text{Diag}(\zeta)$ with $\mathbf{I}_{n_t} \in \mathbb{R}^{n_t \times n_t}$ an identity matrix and $N_{\text{obs}} = n_s n_t$. Here \otimes is the matrix Kronecker product. If the observational noise is temporally uncorrelated, then the covariance Γ_{noise} is generally an $N_{\text{obs}} \times N_{\text{obs}}$ block diagonal matrix $\Gamma_{\text{noise}} = \bigoplus_{m=1}^{n_t} (\mathbf{R}_m)$, where \bigoplus is the matrix direct sum and $\mathbf{R}_m \in \mathbb{R}^{n_s \times n_s}$ models the spatial covariances between observation errors prescribed at time instance t_m . Note that the matrix direct sum is equivalent to the matrix Kronecker product with an identity matrix only if the entries of the direct sum are identical.

If the observation correlations are time independent, namely, $\mathbf{R}_m = \mathbf{R}, \forall m$, then $\Gamma_{\text{noise}} = \mathbf{I}_{n_t} \otimes \mathbf{R}$. In the presence of spatiotemporal correlations, the covariance matrix Γ_{noise} becomes a dense symmetric block matrix with the mn th block \mathbf{R}_{mn} describing covariances between observation gridpoints at time instances t_m and t_n , respectively.

The standard Bayesian OED formulation, discussed above, is ideal for spatially and temporally uncorrelated observation errors. However, it may not properly account for spatiotemporal correlations, and it is harder to apply when the design is allowed to vary over time. Specifically, the role of the relaxed design matrix is to weight covariances between candidate sensor locations—a maximum weight of 1 means activating the corresponding sensors, and a minimum weight of 0 means deactivating them—based on their contribution to the OED optimality objective. Thus, the weighting matrix \mathbf{W} needs to be applied to the observation error covariance matrix, and not to the precision matrix [31], which is initially obtained based on the assumption that all sensors are activated. Moreover, the formulation does not provide enough flexibility for handling the effect of spurious observation correlations that might be introduced, for example, by misspecification of the observational error covariances. Furthermore, it does not provide any control over the values of design, besides

the imposed bound constraints. For example, no inherent property enables imposing preference of specific values of the design variables such as observation cost constraints. In [Section 3](#) we further discuss the issue of relaxation and introduce a generalized formulation of the OED problem capable of handling these limitations.

2.5. The OED optimization problem. The relaxed OED problem for sensor placement is described by the following constrained optimization problem,

$$(2.8) \quad \zeta^{\text{opt}} = \arg \min_{\zeta \in [0, 1]^{n_s}} \mathcal{T}(\zeta) := \Psi(\zeta) + \alpha \Phi(\zeta),$$

where Ψ is the design criterion, $\Phi(\zeta): [0, 1]^{n_s} \mapsto [0, \infty)$ is a penalty function that enforces regularization or sparsity on the design, and $\alpha > 0$ is a user-defined penalty parameter. The optimality criterion Ψ is set to Ψ^{GA} or Ψ^{GD} , defined by [\(2.5\)](#), for obtaining an A- or D-optimal design, respectively.

A gradient-based optimization approach is followed to numerically solve [\(2.8\)](#). A central piece of this procedure is the gradient of the optimality criterion Ψ . For $i = 1, 2, \dots, n_s$, the derivatives of the A- and D-optimality criteria [\(2.5\)](#), respectively, are

$$(2.9a) \quad \frac{\partial \Psi^{\text{GA}}}{\partial \zeta_i} = -\text{Tr} \left(\mathbf{P} \mathbf{H}^{-1}(\zeta) \mathbf{F}^* \frac{\partial \mathbf{W}_\Gamma(\zeta)}{\partial \zeta_i} \mathbf{F} \mathbf{H}^{-1}(\zeta) \mathbf{P}^* \right),$$

$$(2.9b) \quad \frac{\partial \Psi^{\text{GD}}}{\partial \zeta_i} = \text{Tr} \left(\boldsymbol{\Sigma}_{\text{post}}^{-1}(\zeta) \mathbf{P} \mathbf{H}^{-1}(\zeta) \mathbf{F}^* \frac{\partial \mathbf{W}_\Gamma(\zeta)}{\partial \zeta_i} \mathbf{F} \mathbf{H}^{-1}(\zeta) \mathbf{P}^* \right),$$

where $\mathbf{H}(\zeta)$ is the weighted Hessian of the negative log of the posterior PDF, $\mathbf{H}(\zeta) := \boldsymbol{\Gamma}_{\text{pr}}^{-1} + \mathbf{F}^* \mathbf{W}_\Gamma(\zeta) \mathbf{F}$. The gradient of the objective [\(2.8\)](#) is obtained by combining the gradient of the penalty term $\nabla_\zeta \Phi(\zeta)$ with the optimality criterion [\(2.9\)](#), that is, $\nabla_\zeta \mathcal{T}(\zeta) = \nabla_\zeta \Psi(\zeta) + \alpha \nabla_\zeta \Phi(\zeta)$, and is provided to the numerical optimization routine.

The general form of the derivative [\(2.9\)](#) shows that, to formulate the gradient, we need the derivative of the weighted observation precision matrix $\mathbf{W}_\Gamma(\zeta)$. The final form of the gradient depends on the specific form of the weighted observation precision matrix $\mathbf{W}_\Gamma(\zeta)$. Most studies assume uncorrelated observations and derive the gradient accordingly for simplicity. In the next section we provide a generalized formulation of the weighted noise matrix and the OED problem, with emphasis on the effect of the design on the observations and observation spatiotemporal correlations.

Deploying observational sensors can be expensive, and in general we seek a small number of sensors to accurately solve the inverse problem with minimum uncertainty levels. To achieve this goal, we choose the penalty Φ function to enforce sparsity on the optimal design. Sparsification can be achieved by using the ℓ_0 “norm” [\[3\]](#); however, ℓ_0 is not a valid norm and is nondifferentiable, which leads to complications in the optimization procedure. An acceptable level of sparsification can be achieved by utilizing the ℓ_1 norm in the regularization term [\[2\]](#).

The solution of [\(2.8\)](#) is expected to be a sparse design; however, it is not necessarily binary. A binary design can be obtained from the solution of the relaxed optimization problem [\(2.8\)](#), for example, by applying thresholding [\[2, 6\]](#) or by applying a continuation procedure or by reweighting the regularization term [\[27, 30\]](#). Another approach to ensure a binary design is to partition the domain and use the sum-up rounding procedure; see, for example, [\[43, 53\]](#). The simplest approach is to truncate the relaxed optimal design. This can be done by activating sensors corresponding to the nonvanishing weight (e.g., greater than a small-enough value,) resulting from solving the relaxed

OED problem. Alternatively, given a specific budget λ , one can activate the sensors corresponding to the highest λ nonzero weights in the relaxed optimal design.

Following the approach in [2, 6], in the numerical experiments reported in Section 4 we promote sparsification by setting Φ to the ℓ_1 norm. Once a sparse optimal design is obtained, we choose the sensors corresponding to the highest λ optimal weights. Note that the discussion here is not limited by the choice of Φ and can be used with other sparsification methods.

3. OED for Correlated Observations. With observational noise being uncorrelated in space and in time, the mathematical analysis of the traditional formulation of the PDE-constrained OED problem is simple; however, this places limitations on the applicability of the formulated framework. In this section we address this issue by formulating the OED problem where the design choice is sensitive not only to the variances of the involved observational errors but also to the spatiotemporal correlations. Specifically, in this section we introduce a generalization of the traditional OED framework, following a Hadamard product approach [28] for likelihood weighting. This will add another dimension of flexibility that will help us formulate a general OED framework capable of handling observation noise with spatiotemporal correlation. We start with a discussion of the effect of design relaxation in Subsection 3.1, followed by the proposed approach starting from Subsection 3.2.

3.1. Insight into the relaxation of binary OED problem. As discussed in Subsection 2.4, one can define the weighted precision matrix by weighting the precision matrix $\mathbf{\Gamma}_{\text{noise}}^{-1}$ by the design weights.

Precision matrix weighting. In this case we form the weighted precision matrix as $\mathbf{W}_{\Gamma}(\zeta) := \mathbf{W}^{\frac{1}{2}}(\zeta)\mathbf{\Gamma}_{\text{noise}}^{-1}\mathbf{W}^{\frac{1}{2}}$ and then the optimization problem (2.8). To utilize the derivative (2.9) in a gradient-based optimization approach for solving (2.8), one needs to calculate $\frac{\partial \mathbf{W}_{\Gamma}(\zeta)}{\partial \zeta_i}$. However, an issue is that in general the derivative would not be defined at $\zeta_i = 0$. A possible remedy would be to redefine the weighted precision matrix by pre- and postmultiplication with the relaxed design:

$$(3.1) \quad \mathbf{W}_{\Gamma}(\zeta) := \mathbf{W}(\zeta)\mathbf{\Gamma}_{\text{noise}}^{-1}\mathbf{W}(\zeta).$$

In this case one can show that

$$(3.2a) \quad \frac{\partial \mathbf{W}_{\Gamma}(\zeta)}{\partial \zeta_i} = \mathbf{v}_i(\zeta)\mathbf{e}_i^{\top} + \mathbf{e}_i\mathbf{v}_i^{\top}; \quad \mathbf{v}_i(\zeta) = (\mathbf{\Gamma}_{\text{noise}}^{-1}\mathbf{e}_i) \odot \zeta; i = 1, \dots, n_s,$$

where \odot is the pointwise product and \mathbf{e}_i is the i th versor of \mathbb{R}^{n_s} . By substituting (3.2a) in (2.9), the derivatives (for A- and D-optimality) are

$$(3.2b) \quad \frac{\partial \Psi^{\text{GA}}}{\partial \zeta_i} = -2\mathbf{e}_i^{\top}\mathbf{F}\mathbf{H}^{-1}(\zeta)\mathbf{P}^*\mathbf{P}\mathbf{H}^{-1}(\zeta)\mathbf{F}^*\mathbf{v}_i(\zeta),$$

$$(3.2c) \quad \frac{\partial \Psi^{\text{GD}}}{\partial \zeta_i} = -2\mathbf{e}_i^{\top}\mathbf{F}\mathbf{H}^{-1}(\zeta)\mathbf{P}^*\mathbf{\Sigma}_{\text{post}}^{-1}(\zeta)\mathbf{P}\mathbf{H}^{-1}(\zeta)\mathbf{F}^*\mathbf{v}_i(\zeta),$$

where we used the circular and transposition properties of the matrix trace. This can be thought of as an *ad hoc* fix of the standard OED formulation where \mathbf{W} pre- and postmultiply the precision matrix (instead of using $\mathbf{W}^{\frac{1}{2}}$). This raises another problem, however: Even with the ad hoc fix (3.1), this formulation yields a relaxed solution that is not guaranteed to match the solution of the original binary OED problem. The reason is that the weighting is carried out after the precision matrix $\mathbf{\Gamma}_{\text{noise}}^{-1}$

is formulated assuming all sensors are active (even if a design variable is set to 0), and thus inactive sensors contribute to the elements in the precision (inverse covariance) matrix corresponding to active sensors. More formally, it is not guaranteed—unless $\mathbf{\Gamma}_{\text{noise}}$ is diagonal—that $\lim_{\zeta \rightarrow \zeta^b} \mathbf{W}_{\Gamma}(\zeta)$ is equal to the degenerate precision matrix $\mathbf{\Gamma}_{\text{noise}}^{-1}(\zeta^b)$ obtained by eliminating rows/columns from $\mathbf{\Gamma}_{\text{noise}}$ corresponding to zero entries of ζ^b , where $\zeta^b \in \{0, 1\}^{n_s}$. In other words, the matrix $\mathbf{W}_{\Gamma}(\zeta)$ may not have the correct limit as ζ approaches points on the boundary of the relaxed domain $[0, 1]^{n_s}$. This issue will be discussed further below.

Effect of relaxing the design. To properly formulate and solve sensor placement problems, we start by discussing the roles played by the binary design and the associated relaxation. The original OED binary optimization problem for sensor placement takes the form

$$(3.3) \quad \min_{\zeta^b \in \{0, 1\}^{n_s}} \Psi(\zeta^b),$$

where we dropped the regularization term for simplicity. Here, Ψ depends on ζ^b through the weighted precision matrix \mathbf{W}_{Γ} . The binary design $\zeta^b := (\zeta_1^b, \dots, \zeta_{n_s}^b)^{\top}$ characterizes the active sensors and thus defines which entries of the observation vector to keep and which to remove. This corresponds to keeping/removing rows and columns from the observation error covariance matrix $\mathbf{\Gamma}_{\text{noise}}$. As described by (2.6) and (2.7), this is encoded in the inverse problem by modifying the likelihood function. Since we generally assume observation errors are Gaussian, that is, $\delta := \mathbf{y} - \mathbf{F}(\theta) \sim \mathcal{N}(\mathbf{0}, \mathbf{\Gamma}_{\text{noise}})$, one can encode the design in the likelihood as $\mathbf{L}(\mathbf{y} - \mathbf{F}(\theta)) \sim \mathcal{N}(\mathbf{0}, \mathbf{L}\mathbf{\Gamma}_{\text{noise}}\mathbf{L}^{\top})$, where $\mathbf{L} := \mathbf{L}(\zeta^b)$ is a sparse matrix that extracts rows and columns of $\mathbf{\Gamma}_{\text{noise}}$ that correspond to active sensors; that is, $\mathbf{L} := \mathbf{L}(\zeta^b) \in \mathbb{R}^{n_a \times n_s}$, $n_a = \sum \zeta_j^b$, $\mathbf{L}_{ij} = 1$ if ζ_j^b is nonzero. In other words, \mathbf{L} is a binary matrix with only one entry equal to 1 on each row, and the number of rows is equal to the number of active sensors. If we define a binary weight matrix $\mathbf{W}(\zeta^b) := \text{Diag}(\zeta^b)$, then $\mathbf{L}(\zeta^b)[\mathbf{y} - \mathbf{F}(\theta)] \sim \mathcal{N}(\mathbf{0}, \mathbf{L}(\zeta^b)\mathbf{W}(\zeta^b)\mathbf{\Gamma}_{\text{noise}}\mathbf{W}^{\top}(\zeta^b)\mathbf{L}^{\top}(\zeta^b))$, and thus we can write the weighted data likelihood on the form (introducing \mathbf{W} here does not make a difference given the definition of \mathbf{L} , but it will be crucial when the design is relaxed):

$$(3.4) \quad \mathcal{L}(\mathbf{y}|\theta; \zeta) \propto \exp\left(-\frac{1}{2} \|\mathbf{F}\theta - \mathbf{y}\|_{\mathbf{Q}}^2\right); \quad \mathbf{Q} := \mathbf{L}^{\top}(\zeta^b) (\mathbf{L}(\zeta^b)\mathbf{W}(\zeta^b)\mathbf{\Gamma}_{\text{noise}}\mathbf{W}^{\top}(\zeta^b)\mathbf{L}^{\top}(\zeta^b))^{-1} \mathbf{L}(\zeta^b).$$

Note that pre- and postmultiplication of $\mathbf{\Gamma}_{\text{noise}}$ by the diagonal matrix \mathbf{W} means that the (i, j) th entry of $\mathbf{\Gamma}_{\text{noise}}$ is scaled by $\zeta_i^b \zeta_j^b$, where $i, j = 1, \dots, n_s$. Loosely speaking, the effect can be explained as follows. When $\zeta_i^b = 0$, the i th row and column of $\mathbf{\Gamma}_{\text{noise}}$ are set to 0 and are then eliminated by the effect of \mathbf{L} . Inversion of the covariance matrix is carried out in the projected space (by removing data corresponding to that inactive sensor then evaluating the inverse) and the precision matrix is then projected back to the original space by applying the transpose of \mathbf{L} .

LEMMA 3.1. *Let $\mathbf{W} := \text{Diag}(\zeta^b)$, $\zeta^b \in \{0, 1\}^{n_s}$. $\mathbf{\Gamma}_{\text{noise}} \in \mathbb{R}^{n_s \times n_s}$ is an admissible covariance matrix, and \mathbf{L} is as defined above. Then*

$$(3.5) \quad \mathbf{L}^{\top}(\zeta^b) (\mathbf{L}(\zeta^b)\mathbf{W}(\zeta^b)\mathbf{\Gamma}_{\text{noise}}\mathbf{W}^{\top}(\zeta^b)\mathbf{L}^{\top}(\zeta^b))^{-1} \mathbf{L}(\zeta^b) = (\mathbf{W}(\zeta^b)\mathbf{\Gamma}_{\text{noise}}\mathbf{W}^{\top}(\zeta^b))^{\dagger},$$

where \dagger denotes the Moore–Penrose (pseudo) inverse.

Proof. See [Appendix A](#). □

Despite being elementary, the significance of [Lemma 3.1](#) is that it enables rewriting the weighted data likelihood (3.4) in the following equivalent form:

$$(3.6) \quad \mathcal{L}(\mathbf{y}|\theta; \zeta) \propto \exp\left(-\frac{1}{2} \|\mathbf{F}\theta - \mathbf{y}\|_{(\mathbf{W}(\zeta^b)\mathbf{\Gamma}_{\text{noise}}\mathbf{W}^{\text{T}}(\zeta^b))^{\dagger}}^2\right).$$

Let us relax the design variable ζ to take any value in the domain $[0, 1]^{n_s}$, and let the observation errors be uncorrelated, that is, diagonal $\mathbf{\Gamma}_{\text{noise}}$. When the relaxed design attains a corner point of the domain, that is, $\zeta \in \{0, 1\}^{n_s}$, the argument and formulation of the likelihood (3.6) hold. However, this formulation becomes inconsistent for any value of the design in the interior of the relaxation domain, that is, $(0, 1)^{n_s}$. Intuitively speaking, we aim to discard a sensor that does not provide valuable information (e.g., the sensor provides negligible information or is associated with a very high uncertainty level). Now, consider a design value $\zeta = \epsilon \in (0, 1)$; by pre- and postmultiplying the variance of the i th sensor with ϵ . By letting $\epsilon \rightarrow 0$, the posterior becomes sharper (the variance is reduced), which is the exact opposite of the desired behavior.

Naive solution. In general, we need to formulate the relaxed weighted likelihood such that the weighted variance of the i th sensor increases as the associated design $\zeta_i \rightarrow 0$. This can be achieved by replacing the diagonal of the design matrix with weights $w_{i,i}$ defined as

$$(3.7) \quad w_{i,i}(\zeta) = \begin{cases} \frac{1}{\zeta_i} & ; \zeta_i \in (0, 1], \\ 0 & ; \zeta_i = 0, \end{cases} \quad i = 1, \dots, n_s.$$

This way, as $\zeta_i \rightarrow 0$, we weight the sensor such that accuracy of the weighted version decreases. In the case of uncorrelated observational errors, that is, $\mathbf{\Gamma}_{\text{noise}}$ is diagonal, one can show that $(\mathbf{W}\mathbf{\Gamma}_{\text{noise}}\mathbf{W})^{\dagger} = \text{Diag}(\zeta) \mathbf{\Gamma}_{\text{noise}}^{-1} \text{Diag}(\zeta)$, which is the traditional weighting form discussed in [Subsection 2.4](#).

The form (3.7), however, is invalid for correlated observations. Specifically, consider the case when $\mathbf{\Gamma}_{\text{noise}}$ is nondiagonal, that is, the observation errors are correlated. Pre- and postmultiplication of $\mathbf{\Gamma}_{\text{noise}}$ by \mathbf{W} corresponds to weighting the (i, j) entry of $\mathbf{\Gamma}_{\text{noise}}$ by $w_{i,i}w_{j,j}$. More specifically, the design variable ζ_i contributes to the weight of the i th row/column of $\tilde{\mathbf{\Gamma}}_{\text{noise}}(\zeta) := \mathbf{W}(\zeta)\mathbf{\Gamma}_{\text{noise}}\mathbf{W}(\zeta)$. If we define the weights as described by (3.7), then while the variance of the i th sensor increases as $\zeta_i \rightarrow 0$, the correlations between the i th sensors and other sensors are also magnified. However, a less important sensor (to be discarded) should have higher uncertainty and be less correlated with other sensors, and thus the definition in (3.7) becomes invalid.

Note that pre- and postmultiplication of $\mathbf{\Gamma}_{\text{noise}}^{-1}$ with $\mathbf{W} := \text{Diag}(\zeta)$ means that the precision matrix $\mathbf{\Gamma}_{\text{noise}}^{-1}$ is evaluated first assuming that all sensors are active and is then weighted, which results in a discontinuity in the objective at $\zeta = 0$. This can be shown in the context of the following simple two-dimensional example.

Illustration of the issue. Following the definition of the linear forward and inverse problem in [Section 2](#), we define the parameter-to-observable map \mathbf{F} as a short, wide matrix that projects a model parameter/state onto the observation space. The prior and observation covariance matrices are defined, and the posterior covariance matrix $\mathbf{\Gamma}_{\text{post}}$ is then used to formulate the A-optimality criterion Ψ^{GA} as defined by (2.5) with $\mathbf{\Gamma}_{\text{noise}}$ replaced by a weighted version based on the relaxed

design. The forward operator (randomly generated) and prior and observation noise covariances are

$$(3.8) \quad \mathbf{F} := \begin{bmatrix} -0.125 & -0.15 & 1.145 & -0.475 \\ 0.485 & -2.13 & 0.41 & 0.495 \end{bmatrix}; \quad \mathbf{\Gamma}_{\text{noise}} := \begin{bmatrix} 2.0 & 1.0 \\ 1.0 & 2.0 \end{bmatrix} \quad \mathbf{\Gamma}_{\text{pr}} := \mathbf{I},$$

where $\mathbf{I} \in \mathbb{R}^{4 \times 4}$ is an identity matrix, with the following form of the A-optimality criterion:

$$(3.9) \quad \Psi(\zeta) := \Psi^{\text{GA}}(\zeta) = \text{Tr}(\mathbf{\Gamma}_{\text{post}}(\zeta)) = \text{Tr}\left(\left(\mathbf{F}^T \mathbf{W}_{\Gamma}(\zeta) \mathbf{F} + \mathbf{\Gamma}_{\text{pr}}^{-1}\right)^{-1}\right),$$

where (3.6) and (3.7) are utilized to define $\mathbf{W}_{\Gamma}(\zeta)$. The forward operator \mathbf{F} in (3.8) describes a simulation at four model gridpoints, with $n_s = 2$ candidate observational sensors. The first sensor measures the average value simulated at the first two model gridpoints, and the second sensor measures the average value simulated at the last two gridpoints. Figure 1 (left) shows a surface plot of the OED A-optimality criterion as a function of the relaxed design $\zeta \in [0, 1]^2$. The surface plot is evaluated only at points in the interior of the domain $(0, 1)^2$. The value of the optimality criterion evaluated at the binary design values $\zeta^{\text{b}} \in \{0, 1\}^2$, namely, at the corners of the domain, are shown as colored circles. Similar results are obtained when the covariance matrix is pre- and postmultiplied by the design square root, as shown in Figure 1 (right).

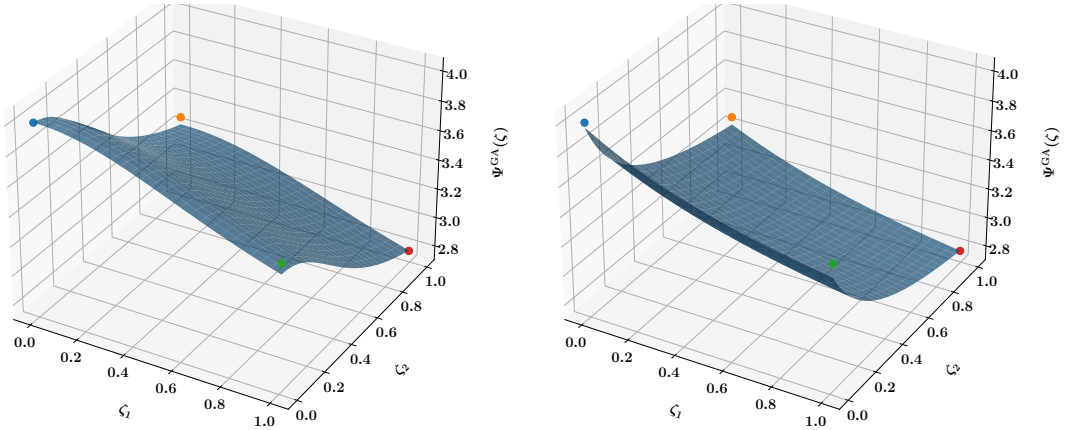


FIG. 1. Values of the OED A-optimality criterion (objective) evaluated at points in the interior of the domain of the relaxed design $(0, 1)^2$, by using $\mathbf{W}_{\Gamma}(\zeta) := (\mathbf{W}(\zeta)\mathbf{\Gamma}_{\text{noise}}\mathbf{W}^T(\zeta))^{\dagger}$ (left) and $\mathbf{W}_{\Gamma}(\zeta) := (\mathbf{W}^{\frac{1}{2}}(\zeta)\mathbf{\Gamma}_{\text{noise}}\mathbf{W}^{\frac{1}{2}}(\zeta))^{\dagger}$ (right), respectively, with $\mathbf{W}(\zeta) := \text{Diag}(\zeta)$. The value of the optimality criterion evaluated at the binary design values $\zeta^{\text{b}} \in \{0, 1\}^2$ is shown as distinct bullets.

Results in Figure 1 show that (3.9) is discontinuous at $(0, 1)^T$, $(1, 0)^T$. While the mismatch in this example is not significant, such discontinuity is sufficient to show that the standard relaxation approaches (precision pre- and postmultiplication or covariance pre- and postmultiplication with the ad hoc fix) are not valid in the case of correlated observations. Specifically, the limit of the relaxed objective, as the design attains a binary value, is not well defined. This leads to discontinuity of the objective, invalidates the associated gradient, and shows that solving a relaxation of the binary OED optimization problem is not guaranteed to produce a design that is either binary or matches the optimal solution of the original binary optimization problem.

3.2. Schur product formulation of the OED problem. To achieve the desired weighting behavior and resolve the issues discussed in [Subsection 3.1](#), we reformulate the weighted likelihood by replacing the covariance matrix $\mathbf{\Gamma}_{\text{noise}}$ with a weighted version $\tilde{\mathbf{\Gamma}}_{\text{noise}}(\zeta) := \mathbf{W}(\zeta) \odot \mathbf{\Gamma}_{\text{noise}}$, where \odot is the Hadamard (Schur) product, $\mathbf{W}_{\Gamma}(\zeta) = \tilde{\mathbf{\Gamma}}_{\text{noise}}^{\dagger}(\zeta)$, and $\mathbf{W}(\zeta)$ is a weighting matrix with entries defined as

$$(3.10) \quad \varpi(t_m, t_n; \zeta_i, \zeta_j) = \begin{cases} w_i(t_m, t_n) w_j(t_m, t_n) & ; i \neq j \\ \begin{cases} 0 & ; w_i(t_m, t_n) = 0 \\ \frac{1}{w_i^2(t_m, t_n)} & ; w_i(t_m, t_n) \neq 0 \end{cases} & ; i = j \end{cases} ; \quad \begin{matrix} i, j = 1, 2, \dots, n_s, \\ m, n = 1, 2, \dots, n_t, \end{matrix}$$

where $w_i(t_m, t_n) \in [0, 1]$ is a weight calculated based on the value of the design ζ_i ; this weight is applied to autocovariances of the i th candidate sensor at time instances t_m, t_n , respectively. Autocovariance here refers to the covariance between observational noise at different time instances for the same observational sensor. For uncorrelated temporal observational errors, the simplest form is to let $w_i(t_m, t_n) := \zeta_i$. The weights given by (3.10) assure that the desired weighting scheme discussed in [Subsection 3.1](#) is achieved by the weighting kernel $\mathbf{W}(\zeta)$. The weighting function $\varpi(t_m, t_n; \zeta_i, \zeta_j)$ is symmetric, and thus the weighting kernel $\mathbf{W}(\zeta)$ itself is a symmetric and doubly nonnegative—real positive semidefinite square matrix—weighting kernel. The symmetry here is defined over any permutation of the time indexes or the design variables. In other words $\varpi(t_m, t_n; \zeta_i, \zeta_j) = \varpi(t_n, t_m; \zeta_i, \zeta_j) = \varpi(t_m, t_n; \zeta_j, \zeta_i) = \varpi(t_n, t_m; \zeta_j, \zeta_i)$.

In the discussion below, we consider time-dependent settings, where the states are checkpointed at the observation times for efficient evaluation and storage of the model state and the adjoints. As explained in [Subsection 4.1](#), checkpointing is crucial for solving large-scale time-dependent Bayesian inverse problems. The case of time-independent models can be viewed as a special case of the temporally uncorrelated setup with one observation time instance. We note that the entries of the observation error covariance matrix $\mathbf{\Gamma}_{\text{noise}}$ describe covariances between all candidate sensor locations, at all observation time instances, as discussed in [Subsection 2.4](#). The general form of the weighting function given by (3.10) enables scaling the entries of the covariance matrix $\mathbf{\Gamma}_{\text{noise}}$, where the respective weights are calculated based on both time and space. We explain this thought using a simplified example. Consider a time-dependent simulation with an observational grid with $n_s = 2$ candidate sensor locations. Assume the observations are to be collected at two time instances t_1, t_2 , respectively, with the observation error covariance matrix

$$\mathbf{\Gamma}_{\text{noise}} = \begin{bmatrix} \mathbf{R}_{1,1} & | & \mathbf{R}_{1,2} \\ \hline \mathbf{R}_{2,1} & | & \mathbf{R}_{2,2} \end{bmatrix},$$

where each block $\mathbf{R}_{n,m} \in \mathbb{R}^{2 \times 2}$ describes the error covariances between observational gridpoints at time instances t_n, t_m , respectively, where $n, m = 1, 2$. The design $\zeta \in \Xi \subseteq \mathbb{R}^2$ is associated with the candidate sensor locations and thus is defined as $\zeta = (\zeta_1, \zeta_2)^{\top}$. The weighting matrix is defined as follows:

$$\mathbf{W}(\zeta) := \begin{bmatrix} \varpi(t_1, t_1; \zeta_1, \zeta_1) & \varpi(t_1, t_1; \zeta_1, \zeta_2) & | & \varpi(t_1, t_2; \zeta_1, \zeta_1) & \varpi(t_1, t_2; \zeta_1, \zeta_2) \\ \varpi(t_1, t_1; \zeta_2, \zeta_1) & \varpi(t_1, t_1; \zeta_2, \zeta_2) & | & \varpi(t_1, t_2; \zeta_2, \zeta_1) & \varpi(t_1, t_2; \zeta_2, \zeta_2) \\ \hline \varpi(t_2, t_1; \zeta_1, \zeta_1) & \varpi(t_2, t_1; \zeta_1, \zeta_2) & | & \varpi(t_2, t_2; \zeta_1, \zeta_1) & \varpi(t_2, t_2; \zeta_1, \zeta_2) \\ \varpi(t_2, t_1; \zeta_2, \zeta_1) & \varpi(t_2, t_1; \zeta_2, \zeta_2) & | & \varpi(t_2, t_2; \zeta_2, \zeta_1) & \varpi(t_2, t_2; \zeta_2, \zeta_2) \end{bmatrix}.$$

This shows that the dimension of the design is independent from the size of the temporal domain and is generally much less than the dimension of the space-time domain. Additionally, this

formulation gives more flexibility in forming the design matrix, which acts as a weighting kernel in the observation space. For example, one can define the design matrix following the approach used to define the covariance weighting kernels in [7]. In fact, this formulation has some similarity with spatial covariance localization widely used in the numerical weather prediction applications to remove spurious correlations in ensemble-based prior covariance matrices. Conversely, here we define a design matrix \mathbf{W} to weight/localize covariances between observational sensors based on their respective contribution to the uncertainty of the inversion parameter. If one believes that the effect of correlation on the design should decay in space or in the presence of spurious correlations in observation errors, one can encode this decay in the definition of the weighting function ϖ , in other words, the entries of the design matrix \mathbf{W} . This formulation will enable us to fix the size of the design space to that of the observation space, even when spatiotemporal correlations are considered, thus reducing the computational cost of solving the OED optimization problem.

If the problem is time independent, the matrix $\mathbf{\Gamma}_{\text{noise}}$ describes the covariances between errors of pairs of candidate sensors. In this case the weighting kernel \mathbf{W} requires a weighting function that depends only on pairs of design variables, that is, $\varpi := \varpi(\zeta_i, \zeta_j)$; and the weighting kernel, described by its respective entries, takes the form $\mathbf{W} = [\varpi(\zeta_i, \zeta_j)]_{i,j=1,2,\dots,n_s}$.

Similarly, if the problem is time dependent, while only space correlations are considered, the weight function $\varpi(t_m, t_n; \zeta_i, \zeta_j)$ vanishes for any two different time instances $t_m \neq t_n$, and the weighting kernel becomes a block diagonal matrix taking the form $\mathbf{W} = \bigoplus_{m=1}^{n_t} ([\varpi(\zeta_i, \zeta_j)]_{i,j=1,2,\dots,n_s})$. Further discussion about the spatial weighting function ω is given in [Subsection 3.3](#).

3.3. On the choice of the weighting function. The value of the weighting function $\varpi(\zeta_i, \zeta_j)$ at any pair of observation gridpoints (and design variables) is used to localize the effect of the correlation between any pair of points. Specifically, $\varpi(\zeta_i, \zeta_j) := \omega(\zeta_i)\omega(\zeta_j)$ scales the (i, j) th entry of the spatial observation error covariance matrix $\mathbf{\Gamma}_{\text{noise}}$. Moreover, when $i = j$, the weighting value scales the uncertainty level of the i th candidate sensor location. We regard the weighting value here in the general sense as a value that indicates the relative importance of each candidate sensor. To formulate the gradient of the optimality criterion with respect to the design, with the range $[0, 1]$, we need to require that the weighting function ω be differentiable. Specifically, in order to control the sparsity of the design, in the optimization problem (2.8) the penalty function $\Phi(\cdot)$ is employed. Assuming, for example, that an ℓ_p norm is used and that $\omega_i \in [0, 1]$ is the weight associated with the i th candidate sensor, we define the penalty function as

$$(3.11) \quad \Phi(\zeta) := \left\| \left(\omega_1, \omega_2, \dots, \omega_{n_s} \right)^T \right\|_p,$$

where the penalty is asserted on the results of the weighting function, regardless of the domain of the design variables themselves. The reason is that the role of the penalty function is to promote sparsity of the design and thus limit the number of activated sensors. Following the discussion in [Subsection 3.1](#), a sensor can be deactivated when it is associated with high uncertainty induced in the posterior and low correlation relative to the other sensors. Thus, sparsification can be achieved by reducing the weights ω_i , which has the effect of reducing the correlation and increasing the uncertainty induced by specific sensors; see the formulation of ϖ given by (3.10). Utilizing (3.11) as a penalty function drives the weights of the sensors to smaller values, which achieves the desired sparsification effect.

As mentioned in [Subsection 3.2](#), the simplest approach is to let $\zeta_i \in [0, 1]$ and define the weight associated with the i th sensor as

$$(3.12) \quad \omega(\zeta_i) \equiv \omega_i := \zeta_i; \quad \frac{\partial \omega(\zeta_i)}{\partial \zeta_k} = \delta_{i,k},$$

where $\delta_{i,k}$ is the Kronecker delta function. The derivative will be used in developing the gradient of the OED optimization objective, as discussed in [Subsection 3.4](#). Alternatively, one can let $\zeta_i \in (-\infty, 0]$ and define the weights as

$$(3.13) \quad \omega(\zeta_i) \equiv \omega_i := e^{\zeta_i}; \quad \frac{\partial \omega(\zeta_i)}{\partial \zeta_k} = \omega_i \delta_{i,k}.$$

Furthermore, one can let $\zeta_i \in \mathbb{R}$ and define the weights using a sigmoid function as

$$(3.14) \quad \omega(\zeta_i) \equiv \omega_i = \frac{1}{1 + e^{-a\zeta_i}}; \quad \frac{\partial \omega(\zeta_i)}{\partial \zeta_k} = a \omega_i (1 - \omega_i) \delta_{i,k},$$

where a is a positive scaling factor (we generally set the scaling coefficient $a = 1$, unless otherwise stated explicitly). The sigmoid function (3.14) frees the design variables to take any real value while keeping the weights in the interval $[0, 1]$ as desired. This will allow utilizing unconstrained optimization approaches to solve the relaxed OED optimization problem.

In the remainder of [Section 3](#) we will keep the discussion independent from the specific choice of the design weighting function ω . We start by formulating and discussing the relaxed OED optimization problem and then discuss the solution approach in two cases. In the first case the observation error covariance matrix is block diagonal with only space correlations ([Subsection 3.5](#)), and in the second case both space and time correlations are allowed ([Subsection 3.6](#)).

3.4. The relaxed OED optimization problem. We utilize the weighted precision matrix $\mathbf{W}_\Gamma(\zeta)$ to formulate the weighted likelihood for OED as follows:

$$(3.15) \quad \mathcal{L}(\mathbf{y}|\theta; \zeta) \propto \exp\left(-\frac{1}{2} \|\mathbf{F}\theta - \mathbf{y}\|_{\mathbf{W}_\Gamma(\zeta)}^2\right); \quad \mathbf{W}_\Gamma(\zeta) := (\mathbf{\Gamma}_{\text{noise}} \odot \mathbf{W}(\zeta))^\dagger,$$

where the weighting kernel $\mathbf{W}(\zeta)$ is constructed using (3.10). Thus, the A- and D-optimal design optimization problems (2.5) take the following respective forms:

$$(3.16a) \quad \zeta^{\text{A-opt}} = \arg \min_{\zeta \in \Xi} \Psi^{\text{GA}}(\zeta) := \text{Tr}\left(\mathbf{P} \left(\mathbf{F}^* (\mathbf{\Gamma}_{\text{noise}} \odot \mathbf{W}(\zeta))^\dagger \mathbf{F} + \mathbf{\Gamma}_{\text{pr}}^{-1}\right)^{-1} \mathbf{P}^*\right),$$

$$(3.16b) \quad \zeta^{\text{D-opt}} = \arg \min_{\zeta \in \Xi} \Psi^{\text{GD}}(\zeta) := \log \det\left(\mathbf{P} \left(\mathbf{F}^* (\mathbf{\Gamma}_{\text{noise}} \odot \mathbf{W}(\zeta))^\dagger \mathbf{F} + \mathbf{\Gamma}_{\text{pr}}^{-1}\right)^{-1} \mathbf{P}^*\right).$$

The remainder of [Subsection 3.4](#) is dedicated to discussing the validity of the proposed formulation both theoretically and empirically. As discussed in [Subsection 2.5](#), in order to numerically solve the optimization problems (3.16), the derivative of the weighted precision matrix $\mathbf{W}_\Gamma(\zeta)$ is required. Thus, before solving the relaxed OED optimization problems (3.16), it is important to show that $\mathbf{W}_\Gamma(\zeta)$ is continuous in ζ and that it converges to the projected precision matrix obtained by using

a binary design. To this end, for clarity we restrict the discussion to the case of spatial correlations, and we consider the case where $w_i := \zeta_i \in [0, 1]$, $i = 1, \dots, n_s$ and show that

$$\mathbf{W}_\Gamma(\zeta) \rightarrow \mathbf{L}^\top(\zeta^b) \left(\mathbf{L}(\zeta^b) \mathbf{\Gamma}_{\text{noise}} \mathbf{L}^\top(\zeta^b) \right)^{-1} \mathbf{L}(\zeta^b),$$

as $\zeta \rightarrow \zeta^b$ for a binary design ζ^b . The other forms of the weights, such as the exponential or sigmoidal weighting kernel, follow similarly since $w_{i,j} \in [0, 1]$. [Lemma 3.2](#) expands the form of the weighted precision matrix \mathbf{W}_Γ and shows similarity with [Lemma 3.1](#).

LEMMA 3.2.

$$(3.17) \quad (\mathbf{\Gamma}_{\text{noise}} \odot \mathbf{W}(\zeta))^\dagger = \mathbf{L}^\top(\zeta) \left(\mathbf{L}(\zeta) \left(\mathbf{\Gamma}_{\text{noise}} \odot \mathbf{W}(\zeta) \right) \mathbf{L}^\top(\zeta) \right)^{-1} \mathbf{L}(\zeta).$$

Proof. See [Appendix A](#). □

The main result here is stated in [Theorem 3.4](#) and shows that the weighted precision $\mathbf{W}_\Gamma(\zeta)$ is continuous and properly relaxes the binary design. The proof of [Theorem 3.4](#) makes use of [Lemma 3.3](#), which shows that the weighting scheme (3.10) is equivalent to regularization of pre- and postmultiplication, as suggested by (A.1). This approach is used to handle discontinuity issues raised for example in c -optimal design problems; see, for example, [41, Section 5.4].

LEMMA 3.3. *Assume $\zeta \in (0, 1)^{n_s}$ and $\mathbf{W}(\zeta)$ is given by (3.10). Then $(\mathbf{W}(\zeta) \odot \mathbf{\Gamma}_{\text{noise}})^{-1} \rightarrow \mathbf{\Gamma}_{\text{noise}}^{-1}$ when $\zeta \rightarrow \mathbf{1}$, and $(\mathbf{W}(\zeta) \odot \mathbf{\Gamma}_{\text{noise}})^{-1} \rightarrow \mathbf{0}$ when $\zeta \rightarrow \mathbf{0}$ where the convergence is elementwise.*

Proof. See [Appendix A](#). □

THEOREM 3.4. *The matrix-valued function $\mathbf{W}_\Gamma(\zeta) = (\mathbf{\Gamma}_{\text{noise}} \odot \mathbf{W}(\zeta))^\dagger$, where ζ is a relaxed design $\zeta \in [0, 1]^{n_s}$ and the entries of the design matrix $\mathbf{W}(\zeta)$ defined by (3.10), is continuous.*

Proof. See [Appendix A](#). □

3.5. Space correlations. Let $\zeta \in \Xi \subseteq \mathbb{R}^{n_s}$ be the design, and assume that the observation errors are temporally uncorrelated. In this case, as discussed in [Subsection 3.2](#), the observation error covariance matrix and the design weighting matrix take the form

$$(3.18) \quad \mathbf{\Gamma}_{\text{noise}} = \bigoplus_{m=1}^{n_t} (\mathbf{R}_m); \quad \mathbf{W} = \bigoplus_{m=1}^{n_t} \left(\sum_{i,j=1}^{n_s} \varpi(\zeta_i, \zeta_j) \mathbf{e}_i \mathbf{e}_j^\top \right),$$

where \mathbf{e}_i is the i th versor of \mathbb{R}^{n_s} , that is, the i th vector in the natural basis. In this case the derivative of \mathbf{W} with respect to a given entry of the design vector, ζ_j , is a sparse symmetric matrix with only nonzero entries in the j th row and the j th column of each block. Specifically, if we define the vector of elementwise partial derivatives of weights

$$(3.19) \quad \eta_j := \left(\frac{\eta_j^{(1)}}{1 + \delta_{1,j}}, \dots, \frac{\eta_j^{(n_s)}}{1 + \delta_{n_s,j}} \right)^\top; \quad \eta_j^{(i)} := \begin{cases} \frac{\partial w_i}{\partial \zeta_i} w_j & ; i \neq j \\ 0 & ; w_i = 0 \\ \frac{-2}{w_i^3} \frac{\partial w_i}{\partial \zeta_i} & ; w_i \neq 0 \end{cases}; \quad i, j = 1, \dots, n_s,$$

which is obtained by piecewise differentiation of (3.10), then it immediately follows that

$$(3.20) \quad \frac{\partial \mathbf{W}_\Gamma(\zeta)}{\partial \zeta_j} = -\mathbf{W}_\Gamma(\zeta) \bigoplus_{m=1}^{n_t} \left(\mathbf{e}_j \left((\mathbf{R}_m \mathbf{e}_j) \odot \eta_j \right)^\top + \left((\mathbf{R}_m \mathbf{e}_j) \odot \eta_j \right) \mathbf{e}_j^\top \right) \mathbf{W}_\Gamma(\zeta),$$

where we utilized the distributive property of the Hadamard product and the fact that \mathbf{R}_m is symmetric and $\mathbf{R}_k \odot (\eta_j \mathbf{e}_j^\top) = ((\mathbf{R}_k \mathbf{e}_j) \odot \eta_j) \mathbf{e}_j^\top$. From (3.15), it follows that

$$(3.21) \quad \mathbf{W}_\Gamma(\zeta) = \bigoplus_{m=1}^{n_t} (\mathbf{V}_m^\dagger(\zeta)), \quad \mathbf{V}_m(\zeta) := \mathbf{R}_m \odot \left(\sum_{i,j=1}^{n_s} \varpi(\zeta_i, \zeta_j) \mathbf{e}_i \mathbf{e}_j^\top \right),$$

where the pseudo inverse in (3.21) can be efficiently evaluated given the fact that $\mathbf{V}_m^\dagger(\zeta) = \mathbf{L}_m^\top (\mathbf{L}_m \mathbf{V}_m(\zeta) \mathbf{L}_m^\top)^{-1} \mathbf{L}_m$, where \mathbf{L}_m extracts the rows/columns from \mathbf{R}_m corresponding to active sensors and all are equal; that is, $\mathbf{L}_k = \mathbf{L}_\ell$, $\forall k, \ell = 1, \dots, n_t$. Note that (3.10) and (3.19) contain terms inversely proportional to the second and third powers of the weights w_i , respectively. These terms tend to infinity as w_i approaches zero, which may yield numerical problems unless handled properly in the software implementation. Thus, a robust implementation of this formulation requires handling such difficulty. The simplest approach is to apply proper rounding to very small weights which can, for example, be encoded in \mathbf{L} . Given the general form of the derivative (2.9), the gradients of the A- and D-optimality criteria (2.5), in the case of temporally uncorrelated observation errors, take the following respective forms (detailed derivation is given in Appendix B.1, Appendix C.1):

$$(3.22a) \quad \nabla_\zeta \Psi^{\text{GA}}(\zeta) = 2 \sum_{m=1}^{n_t} \text{diag} \left(\mathbf{V}_m^\dagger(\zeta) \mathbf{F}_{0,m} \mathbf{H}^{-1}(\zeta) \mathbf{P}^* \mathbf{P} \mathbf{H}^{-1}(\zeta) \mathbf{F}_{m,0}^* \mathbf{V}_m^\dagger(\zeta) (\mathbf{R}_m \odot \mathbf{W}') \right),$$

$$(3.22b) \quad \nabla_\zeta \Psi^{\text{GD}}(\zeta) = 2 \sum_{m=1}^{n_t} \text{diag} \left(\mathbf{V}_m^\dagger(\zeta) \mathbf{F}_{0,m} \mathbf{H}^{-1}(\zeta) \mathbf{P}^* \boldsymbol{\Sigma}_{\text{post}}^{-1}(\zeta) \mathbf{P} \mathbf{H}^{-1}(\zeta) \mathbf{F}_{m,0}^* \mathbf{V}_m^\dagger(\zeta) (\mathbf{R}_m \odot \mathbf{W}') \right),$$

where $\text{diag}(\mathbf{A})$ is the diagonal of a square matrix \mathbf{A} , $\mathbf{F}_{m,0}^*$ is the adjoint of $\mathbf{F}_{0,m}$, and \mathbf{W}' is a matrix with columns set by using (3.19); that is,

$$(3.23) \quad \mathbf{W}' = [\eta_1, \eta_2, \dots, \eta_{n_s}].$$

If we assume a diagonal observational error covariance matrix $\boldsymbol{\Gamma}_{\text{noise}}$ and utilize the kernel (3.12), then the matrix of the derivative reduces to $\mathbf{W}' = \frac{1}{2} \mathbf{I}$. In this case the gradient of the A-optimality criterion (3.22a) and the gradient of the D-optimality criterion (3.22a), respectively, reduce to

$$(3.24a) \quad \nabla_\zeta \Psi^{\text{GA}}(\zeta) = \sum_{m=1}^{n_t} \sum_{i=1}^{N_{\text{goal}}} \mathbf{s}_{i,m} \odot \mathbf{s}_{i,m}; \quad \nabla_\zeta \Psi^{\text{GD}}(\zeta) = \sum_{m=1}^{n_t} \sum_{i=1}^{N_{\text{goal}}} \tilde{\mathbf{s}}_{i,m} \odot \tilde{\mathbf{s}}_{i,m},$$

$$(3.24b) \quad \mathbf{s}_{i,m} := \left(\text{Diag}(\zeta) \mathbf{R}_m^{\frac{1}{2}} \right)^\dagger \mathbf{F}_{0,m} \mathbf{H}^{-1}(\zeta) \mathbf{P}^* \mathbf{e}_i,$$

$$(3.24c) \quad \tilde{\mathbf{s}}_{i,m} := \left(\text{Diag}(\zeta) \mathbf{R}_m^{\frac{1}{2}} \right)^\dagger \mathbf{F}_{0,m} \mathbf{H}^{-1}(\zeta) \mathbf{P}^* \boldsymbol{\Sigma}_{\text{post}}^{-\frac{1}{2}}(\zeta) \mathbf{e}_i,$$

where we utilized the following Lemma 3.5, which can be proven with elementary linear algebra.

LEMMA 3.5. *Given a symmetric matrix \mathbf{A} and a nonnegative diagonal matrix \mathbf{B} such that $\mathbf{A}, \mathbf{B} \in \mathbb{R}^{n \times n}$, then $\text{diag}(\mathbf{A} \mathbf{A}^\top \mathbf{B}) = \text{diag}(\mathbf{B}^{\frac{1}{2}} \mathbf{A} \mathbf{A} \mathbf{B}^{\frac{1}{2}}) = \sum_{i=1}^n \mathbf{s}_i \odot \mathbf{s}_i$; where $\mathbf{s}_i = \mathbf{B}^{\frac{1}{2}} \mathbf{A} \mathbf{e}_i$.*

Note that in this case, that is, when \mathbf{R}_m are diagonal, by utilizing the weighting kernel (3.12) $\varpi(\zeta_i, \zeta_j) := \zeta_i \zeta_j$ we retrieve the standard OED formulation:

$$(3.25) \quad \mathbf{W}_\Gamma = \bigoplus_{m=1}^{n_t} \left(\left((\text{Diag}(\zeta))^\dagger \mathbf{R}_m (\text{Diag}(\zeta))^\dagger \right)^\dagger \right) = \bigoplus_{m=1}^{n_t} (\text{Diag}(\zeta) \mathbf{R}_m^{-1} \text{Diag}(\zeta)).$$

This shows that the traditional OED formulation (for uncorrelated observational errors) is equivalent to applying a Hadamard product weighting kernel to the observation covariance matrix.

Generally speaking, the proposed formulation reduces to the standard OED approach only if the observation errors are uncorrelated and the symmetric kernel function utilized is separable, that is, $\omega(\zeta_i, \zeta_j) = g(\zeta_i)g(\zeta_j)$ for some function $g_*(\zeta_*) : \Omega \subseteq \mathbb{R} \rightarrow [0, 1]$. In this case the weighted precision matrix can be written as

$$\mathbf{W}_\Gamma = \left(\text{Diag}(g(\zeta_1), g(\zeta_2), \dots, g(\zeta_{n_s})) \mathbf{\Gamma}_{\text{noise}} \text{Diag}(g(\zeta_1), g(\zeta_2), \dots, g(\zeta_{n_s})) \right)^{-1}.$$

Note that the gradients (3.22) are well defined only if (3.20) is continuous. This is stated in Lemma 3.6.

LEMMA 3.6. *The matrix-valued entrywise derivative (3.20) is continuous over the relaxation domain $\zeta \in [0, 1]^{n_s}$.*

Proof. See Appendix A. □

We conclude this subsection with an empirical validation. Specifically, we validate the formulation of the relaxed objective (3.16) and derivative (3.22) empirically using the two-dimensional problem Equation (3.8). Figure 2 shows a surface plot (left) of the relaxed objective $\Psi^{\text{GA}}(\zeta)$ described by (3.16a), and a vector-field plot (right) of the gradient (3.22a) evaluated at the discretization point of the relaxed design space. The results show that the relaxation produces a surface that properly connects the corner points that represent the possible values of the binary design. Moreover, the gradient shows continuity in the whole domain including near the boundaries when any of the design variables attain a binary value.

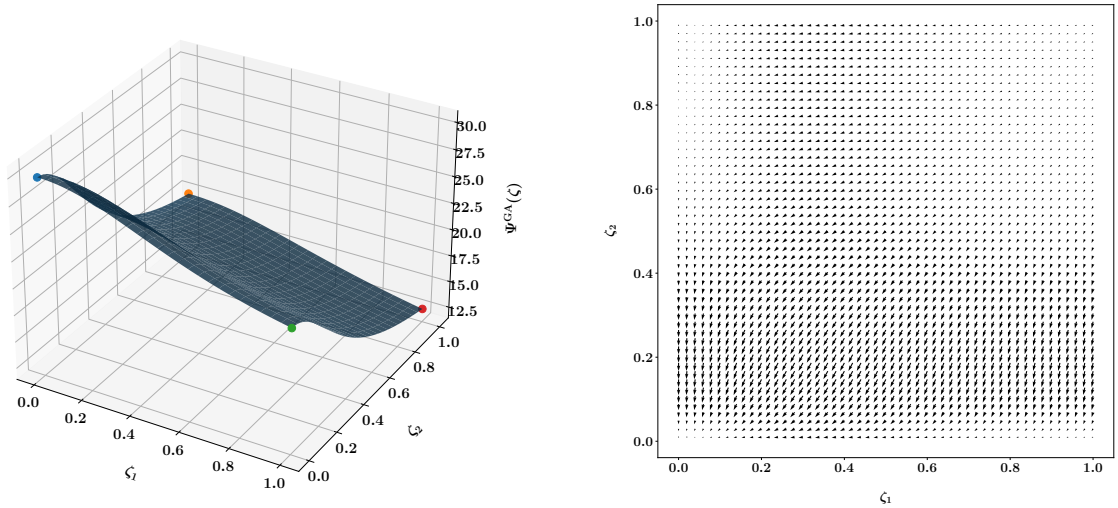


FIG. 2. *Left: values of the OED A-optimality objective (3.16a) evaluated at points in the interior and at the boundaries of the domain of the relaxed design $(0, 1)^2$. The values of the objective evaluated at the binary design values $\zeta^b \in \{0, 1\}^2$ are shown as colored circles. Right: a quiver plot showing a vector-field representation of the gradient (3.22a) evaluated at the discretization point of the relaxed design space (including boundary points).*

3.6. Spatiotemporal correlations. In time-dependent problems, when the observation errors are temporally correlated, the observation noise covariance $\mathbf{\Gamma}_{\text{noise}}$ is a full symmetric matrix, with blocks \mathbf{R}_{mn} representing cross-covariances between observation errors at time instances t_n and t_m , respectively. In space-time settings, one can associate a design variable $\zeta_{i,m}$ for the i th candidate sensor, from n_s candidate locations, at time instance t_m . In this case, however, the design space $\mathbb{R}^{n_s \times n_t}$ grows with the number of observation time instances n_t , and the decision-making process (e.g., thresholding) will be harder to carry out or even interpret. An alternative approach is to associate a design variable ζ_i with the i th candidate sensor location, while controlling its effect in space and over time. For example, we can fix the design variable ζ_i over time, that is, $\zeta_i = \zeta_{i,m}$, $\forall m = 1, 2, \dots, n_t$, while controlling its effect by using the form of ω and by introducing a temporal decorrelation function.

In the majority of time-dependent applications, the temporal correlation strength generally decays in time. In some applications, the correlation between distant temporal points is dominated by spurious correlations, and their effect on the design should be damped out. In this case, in order to choose an optimal design, the temporal effect of a design weight for a candidate sensor location should also decay in time to damp down the effect of spurious correlations on the design selection. For example, one could use $\varpi(\zeta_i, \zeta_j; \cdot, \cdot) := \rho(t_m, t_n) \varpi(\zeta_i, \zeta_j; \cdot, \cdot)$ to weight the entries of \mathbf{R}_{mn} , where, as before, $\varpi(\cdot)$ is a space weighting function and $\rho(t_m, t_n)$ is a symmetric function such that $\rho(t_m, t_m) = 1$ and is conversely related with the distance between t_m and t_n . In this case the entries of $\mathbf{\Gamma}_{\text{noise}}$ are weighted by

$$(3.26) \quad \varpi(\zeta_i, \zeta_j; t_m, t_n) := \begin{cases} \rho(t_m, t_n) \omega(\zeta_i) \omega(\zeta_j) & ; i \neq j \\ \begin{cases} 0 & ; \omega(\zeta_i) = 0 \\ \frac{\rho(t_m, t_n)}{\omega(\zeta_i)^2} & ; \omega(\zeta_i) \neq 0 \end{cases} & ; i = j \end{cases} ; \begin{matrix} i, j = 1, 2, \dots, n_s, \\ k, l = 1, 2, \dots, n_t, \end{matrix}$$

where, as before, $\omega_i \equiv \omega(\zeta)$ is the weight associated with the i th candidate sensor. One could use a Gaussian-like decorrelation function

$$(3.27) \quad \rho(t_m, t_n) := \exp(-d(t_m, t_n)/2\ell^2),$$

where $d(t_m, t_n)$ is a distance function between time instances t_m and t_n and where ℓ is a predefined temporal-correlation length scale. An alternative choice of the weighting coefficients is to employ the fifth-order piecewise-rational function (3.28) of Gaspari and Cohn [22]:

$$(3.28) \quad \rho(t_m, t_n) = \begin{cases} -\frac{v^5}{4} + \frac{v^4}{2} + \frac{5v^3}{8} - \frac{5v^2}{3} + 1, & 0 \leq v \leq 1 \\ \frac{v^5}{12} - \frac{v^4}{2} + \frac{5v^3}{8} + \frac{5v^2}{3} - 5v + 4 - \frac{2}{3v}, & 1 \leq v \leq 2 \\ 0, & 2 \leq v, \end{cases}$$

where $v := \frac{d(t_m, t_n)}{\ell}$ and, as before, ℓ is a predefined correlation length scale and $d(t_n, t_m)$ measures the temporal distance between time instances t_n, t_m . The simplest choice of such a temporal distance function is the Euclidean distance, defined as $d(t_m, t_n) := |t_m - t_n|$. Note that the parameter ℓ here controls the speed at which the decorrelation decays over time, and this should be application specific. The function (3.28) is designed to have compact support such that it is nonzero only for a small local region and zero everywhere else and is used for covariance localization in the data assimilation context; see, for example, [26, 51, 7, 33].

Note that this function is independent from the design variable ζ and is introduced for flexibility, for example, to damp out spurious correlations. One can simply choose $\rho(t_m, t_n) = 1$ if the observation error correlations are correctly specified at all scales. The discussion below is independent from the choice of the temporal weighting function ρ .

In space-time settings, the weighted version of the space-time observation error precision matrix takes the form $\mathbf{W}_\Gamma(\zeta) = (\mathbf{\Gamma}_{\text{noise}} \odot \mathbf{W}(\zeta))^\dagger$, with the space-time weighting matrix $\mathbf{W}(\zeta)$ defined, elementwise, as

$$(3.29) \quad \mathbf{W}(\zeta) := \left[\varpi \left(\zeta_{(k-1) \bmod n_s + 1}, \zeta_{(h-1) \bmod n_s + 1}; t_{\lfloor \frac{k-1}{n_t} \rfloor + 1}, t_{\lfloor \frac{h-1}{n_t} \rfloor + 1} \right) \right]_{k,h=1,2,\dots,N_{\text{obs}}},$$

where $\lfloor \cdot \rfloor$ is the floor operation and \bmod represents the modulo operation. Note that the entrywise representation of the weighting kernel (3.29) shows that the design variables are time independent.

The derivative of the optimality criterion, required for the gradient-based solution of the OED problem, follows directly once the matrix derivative of the weight matrix $\mathbf{W}(\zeta)$ in (3.29) is formulated. To this end, let us define the vector of partial derivatives $\vartheta_{k,n} \in \mathbb{R}^{N_{\text{obs}}}$, $N_{\text{obs}} = n_s \times n_t$, with the k th entry denoted as $\vartheta_{i,m}[k]$ and given by

$$(3.30) \quad \vartheta_{i,m}[k] := \frac{1}{1 + \delta_{i,(k-1) \bmod n_s + 1}} \frac{\partial}{\partial \zeta_i} \varpi \left(\zeta_i, \zeta_{(k-1) \bmod n_s + 1}; t_m, t_{\lfloor \frac{k-1}{n_t} \rfloor + 1} \right); \quad \begin{array}{l} i = 1, \dots, n_s, \\ m = 1, \dots, n_t, \\ k = 1, \dots, N_{\text{obs}}, \end{array}$$

where the piecewise partial derivatives in (3.30) are evaluated using (3.19). The partial derivative of the weight matrix $\mathbf{W}(\zeta)$ with respect to the design variable ζ_i is a symmetric matrix given by

$$(3.31) \quad \frac{\partial \mathbf{W}(\zeta)}{\partial \zeta_i} = \sum_{m=1}^{n_t} \mathbf{e}_q \vartheta_{i,m}^\top + \sum_{m=1}^{n_t} \vartheta_{i,m} \mathbf{e}_q^\top, \quad q = i + (m-1)n_s; \quad i = 1, 2, \dots, n_s,$$

where \mathbf{e}_q here is the q th natural basis vector in $\mathbb{R}^{N_{\text{obs}}}$. By applying the distributive property of the Hadamard product, the partial derivatives of the weighted precision matrix take the form

$$(3.32) \quad \frac{\partial \mathbf{W}_\Gamma(\zeta)}{\partial \zeta_i} = -\mathbf{W}_\Gamma(\zeta) \left(\sum_{m=1}^{n_t} \mathbf{e}_q ((\mathbf{\Gamma}_{\text{noise}}^{-1} \mathbf{e}_q) \odot \vartheta_{i,m})^\top + \sum_{m=1}^{n_t} ((\mathbf{\Gamma}_{\text{noise}}^{-1} \mathbf{e}_q) \odot \vartheta_{i,m}) \mathbf{e}_q^\top \right) \mathbf{W}_\Gamma(\zeta).$$

Given (3.32, 3.30) and, as shown in (Appendix B.2, Appendix B.2), in the presence of spatiotemporal observation correlations, the gradient of the A- and D-optimality criteria take the following respective forms:

$$(3.33a) \quad \nabla_\zeta \Psi^{\text{GA}}(\zeta) = 2 \sum_{i=1}^{n_s} \sum_{m=1}^{n_t} \mathbf{e}_i \mathbf{e}_q^\top \mathbf{W}_\Gamma(\zeta) \mathbf{F} \mathbf{H}^{-1}(\zeta) \mathbf{P}^* \mathbf{P} \mathbf{H}^{-1}(\zeta) \mathbf{F}^* \mathbf{W}_\Gamma(\zeta) ((\mathbf{\Gamma}_{\text{noise}}^{-1} \mathbf{e}_q) \odot \vartheta_{i,m}),$$

$$(3.33b) \quad \nabla_\zeta \Psi^{\text{GD}}(\zeta) = 2 \sum_{i=1}^{n_s} \sum_{m=1}^{n_t} \mathbf{e}_i (\mathbf{\Gamma}_{\text{noise}}^{-1} \mathbf{e}_q \odot \vartheta_{i,m})^\top \mathbf{W}_\Gamma(\zeta) \mathbf{F} \mathbf{H}^{-1}(\zeta) \mathbf{P}^* \Sigma_{\text{post}}^{-1}(\zeta) \mathbf{P} \mathbf{H}^{-1}(\zeta) \mathbf{F}^* \mathbf{W}_\Gamma(\zeta) \mathbf{e}_q.$$

3.7. Computational considerations. The OED objective function and the associated gradient together form the main bottleneck in the process of an OED optimization problem. Evaluating the objective function \mathcal{T} of the OED optimization problem (2.8) and the associated gradient requires evaluating the optimality criterion Ψ and the associated gradient. They also require specifying the penalty function Φ . The cost of evaluating the penalty function and the associated gradient, with respect to the design parameter, is negligible, however, compared with the cost of evaluating Ψ and the associated gradient. Thus, in what follows we focus on the cost of the A-optimality criterion and the associated gradient in terms of the number of forward model evaluations. The analysis extends easily to other optimality criteria including D-optimality.

For simplicity, we assume that the prediction operator \mathbf{P} and the corresponding adjoint \mathbf{P}^* each require one forward model evaluation. The A-optimality criterion $\zeta^{\text{A-opt}}$ described by (2.5) requires one Hessian solve, a forward, and an adjoint integration of the model \mathbf{F} for each entry of the posterior covariance matrix diagonal. The Hessian, being the inverse of the posterior covariance of the model parameter θ , is a function of the relaxed design; see, for example, [6] for details.

A preconditioned conjugate gradient (CG) method is used for Hessian solves, which requires a forward and an adjoint model evaluation for each application of the Hessian. We use the prior covariance as a preconditioner. In this case, and by assuming the numerical rank of the prior preconditioned data misfit Hessian [13] is $r \ll N_{\text{state}}$, then one Hessian solve costs $\mathcal{O}(r)$ CG iterations, that is, $\mathcal{O}(2r)$ forward model evaluations. Thus, one evaluation of the objective function \mathcal{T} in (2.8), assuming A-optimality, costs $\mathcal{O}(2r N_{\text{goal}} + 2 N_{\text{goal}}) = \mathcal{O}(2r N_{\text{goal}})$ forward model solves.

In the case of space correlations, evaluating the gradient of the A-optimality criterion, as described by (3.24a), requires one Hessian solve and two applications of the forward model (including one evaluation of the prediction operator) for each vector in the natural basis $\mathbb{R}^{N_{\text{goal}}}$ at each time instance. Thus, the cost of evaluating the gradient $\nabla_{\zeta} \Psi^{\text{GA}}(\zeta)$ is $\mathcal{O}(2r n_t N_{\text{goal}} + 2 n_t N_{\text{goal}}) = \mathcal{O}(r n_t N_{\text{goal}})$. Similarly, in the case of spatiotemporal correlations, evaluating the gradient (3.33a) costs $\mathcal{O}(n_s n_t (4r + 4)) = \mathcal{O}(4r n_t n_s)$ evaluations of the forward model \mathbf{F} .

3.8. Efficient computation of OED objective and gradient. Solving the OED optimization problem requires repeated evaluation of the trace of the posterior covariance matrix. Moreover, as discussed in Subsection 3.7, constructing the gradient of the optimality criterion requires many forward and backward evaluations of the numerical model, with the computational cost dominated by the cost of evaluating the Hessian matrix \mathbf{H} . To reduce the computational cost, we approximate the Hessian by a randomized approximation of the eigenvalues of a Hermitian matrix as described in [44]; see Appendix D.1 for details. Note that the Hessian matrix \mathbf{H} is never constructed in practice; alternatively, only the effect of its inverse on a vector $\mathbf{H}^{-1}\mathbf{x}$ is required.

Here we discuss using randomized approaches to approximate the optimality criterion for efficient calculation of both the objective and its gradient. Specifically, we utilize a randomized approximation of the matrix trace for A-optimal designs, and we defer the discussion of randomized approximation of the D-optimality criterion to future work.

Given a covariance matrix \mathbf{C} , one can estimate its trace following a Monte Carlo approach, using the relation $\text{Tr}(\mathbf{C}) = \mathbb{E}[\mathbf{z}^T \mathbf{C} \mathbf{z}] \approx \sum_{r=1}^{n_r} \mathbf{z}_r^T \mathbf{C} \mathbf{z}_r$, where $\{\mathbf{z}_r\}_{r=1,2,\dots,n_r}$ are sampled from the distribution of \mathbf{z} , which is generally an i.i.d. random variable that follows a specific probability distribution. The most commonly used are Gaussian and Rademacher distributions [11]. The development of the criterion below is independent from the choice of the probability distribution. In the numerical

experiments, however, we resort to the Hutchinson trace estimator where the samples \mathbf{z}_i are drawn from the Rademacher distribution.

An approximate A-optimality criterion $\tilde{\Psi}^{\text{GA}}(\zeta) \approx \Psi^{\text{GA}}(\zeta)$ takes the form

$$(3.34) \quad \tilde{\Psi}^{\text{GA}}(\zeta) = \frac{1}{n_r} \sum_{r=1}^{n_r} \mathbf{z}_r^\top \boldsymbol{\Sigma}_{\text{post}}(\zeta) \mathbf{z}_r = \frac{1}{n_r} \sum_{r=1}^{n_r} \mathbf{z}_r^\top \mathbf{P} (\mathbf{F} \mathbf{W}_\Gamma(\zeta) \mathbf{F}^* + \boldsymbol{\Gamma}_{\text{pr}}^{-1})^{-1} \mathbf{P}^* \mathbf{z}_r,$$

with $\mathbf{z}_r \in \mathbb{R}^{N_{\text{goal}}}$, and $\mathbf{W}_\Gamma(\zeta)$ is given by (3.15). The derivative of this randomized A-optimality criterion with respect to the i th design variable, where $i = 1, 2, \dots, n_s$, is

$$(3.35) \quad \frac{\partial \tilde{\Psi}^{\text{GA}}(\zeta)}{\partial \zeta_i} = \frac{1}{n_r} \sum_{r=1}^{n_r} \mathbf{z}_r^\top \mathbf{P} \mathbf{H}^{-1}(\zeta) \mathbf{F}^* \mathbf{W}_\Gamma(\zeta) \left(\boldsymbol{\Gamma}_{\text{noise}} \odot \frac{\partial \mathbf{W}(\zeta)}{\partial \zeta_i} \right) \mathbf{W}_\Gamma(\zeta) \mathbf{F} \mathbf{H}^{-1}(\zeta) \mathbf{P}^* \mathbf{z}_r.$$

If we assume that the observations are temporally uncorrelated, the gradient takes the following form (see Appendix B.3 for details):

$$(3.36) \quad \nabla_\zeta \tilde{\Psi}^{\text{GA}}(\zeta) = \frac{2}{n_r} \sum_{r=1}^{n_r} \sum_{m=1}^{n_t} \psi_{r,m}^* \odot ((\mathbf{R}_m \odot \mathbf{W}') \psi_{r,m}); \quad \begin{aligned} \psi_{r,m} &:= \mathbf{V}_m^\dagger(\zeta) \mathbf{F}_{0,m} \mathbf{H}^{-1}(\zeta) \mathbf{P}^* \mathbf{z}_r, \\ \psi_{r,m}^* &:= (\mathbf{z}_r^\top \mathbf{P} \mathbf{H}^{-1}(\zeta) \mathbf{F}_{m,0}^* \mathbf{V}_m^\dagger(\zeta))^\top. \end{aligned}$$

In the presence of spatiotemporal correlations, the gradient is (see Appendix B.3)

$$(3.37) \quad \nabla_\zeta \tilde{\Psi}^{\text{GA}}(\zeta) = 2 \sum_{r=1}^{n_r} \sum_{i=1}^{n_s} \sum_{m=1}^{n_t} \mathbf{e}_i \psi_r^* \mathbf{e}_q ((\boldsymbol{\Gamma}_{\text{noise}} \mathbf{e}_q) \odot \vartheta_{i,m})^\top \psi_r; \quad \begin{aligned} \psi_r &:= \mathbf{W}_\Gamma(\zeta) \mathbf{F} \mathbf{H}^{-1}(\zeta) \mathbf{P}^* \mathbf{z}_r, \\ \psi_r^* &:= \mathbf{z}_r^\top \mathbf{P} \mathbf{H}^{-1}(\zeta) \mathbf{F}^* \mathbf{W}_\Gamma(\zeta). \end{aligned}$$

4. Numerical Experiments. We use an advection-diffusion model to simulate the transport of a contaminant field $u(\mathbf{x}, t)$ in a closed domain \mathcal{D} . A set of candidate sensor locations are predefined, at which the contaminant is to be measured at specific locations in the domain at predefined time instances. The end goal is to predict the concentration of the contaminant at a future time instance, beyond the simulation time. To achieve this goal, first we need to find the *optimal* subset of sensors, from the candidate locations, to deploy a small number of sensors. Here, we define optimality in the sense of A-optimal designs.

4.1. Problem setup. In this section we describe in detail the setup of the numerical experiments carried out in this work.

4.1.1. Model: advection-diffusion. The governing equation of the contaminant $u(\mathbf{x}, t)$ is

$$(4.1) \quad \begin{aligned} u_t - \kappa \Delta u + \mathbf{v} \cdot \nabla u &= 0 & \text{in } \mathcal{D} \times [0, T], \\ u(x, 0) &= \theta & \text{in } \mathcal{D}, \\ \kappa \nabla u \cdot \mathbf{n} &= 0 & \text{on } \partial \mathcal{D} \times [0, T], \end{aligned}$$

where $\kappa > 0$ is the diffusivity, T is the simulation final time, and \mathbf{v} is the velocity field. The domain \mathcal{D} , sketched in Figure 3(left), is the region $(0, 1) \times (0, 1)$, where the rectangular regions model two buildings \mathbf{B}_1 , \mathbf{B}_2 , respectively. The interior of these rectangular regions is excluded from the domain \mathcal{D} , and the contaminant is not allowed to enter. The boundary $\partial \mathcal{D}$ includes both the external

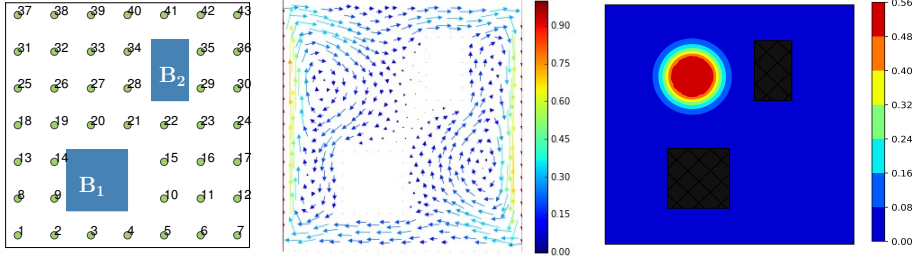


FIG. 3. Advection-diffusion model domain, candidate sensor locations, velocity field, and ground truth of the model parameter. Left: the physical domain \mathcal{D} , including outer boundary, and the two buildings \mathbf{B}_1 , \mathbf{B}_2 . The small circles indicate candidate sensor locations; the sensors are annotated based on their ordering in an observation vector. Middle: the velocity field, which is assumed to be fixed over time. Right: ground truth of the model parameter, in other words, the true value of the model initial condition θ .

boundary and the building walls. The velocity field \mathbf{v} is obtained by solving a steady Navier–Stokes equation, with the side walls driving the flow, as detailed in [39], and is shown in Figure 3(middle). We consider $\kappa > 0$ and \mathbf{v} to be known exactly.

In this work we develop an implementation that utilizes the package HippyLib [50], which provides the forward operator \mathbf{F} , the adjoint \mathbf{F}^* , and a reduced-order Hessian approximation [3]; see Appendix D.1 for additional details on the reduced-order Hessian approximation. We follow the approach in [14], to discretize and simulate the flow PDE (4.1). Specifically, we use finite elements, with Lagrange triangular elements of order 2, with $N_{\text{state}} = 7863$ spatial degrees of freedom in space, and using implicit Euler for simulation in time. The true initial model parameter (shown in Figure 3(right)) is used to create a reference trajectory and synthetic observations.

4.1.2. Observations and observation noise. The contaminant is observed at a set of (candidate) observation gridpoints uniformly distributed in the space domain $\{\mathbf{x}_1, \dots, \mathbf{x}_{n_s}\} \subset \mathcal{D}$, at fixed time instances $\{t_1, t_2, \dots, t_{n_t}\} \subset [0, T]$. The candidate sensor locations, shown in Figure 3(left), constitute the observational grid, with $n_s = 43$ candidate sensor locations. The observation operator \mathcal{B}_k here is a restriction operator applied to the solution $u(\mathbf{x}, t)$ to extract solution values (i.e., concentration of the contaminant) at the predefined observation gridpoints at any time instance t_k . Here the observation times are $t_1 + s\Delta t$, with initial observation time $t_1 = 1$; $\Delta t = 0.2$ is the model simulation time step; and $s = 0, 1, \dots, 5$, resulting in $n_t = 6$ observation time instances. The matrix representation of the observation operator \mathcal{B}_k at any time instance t_k is plotted in Figure 4(left).

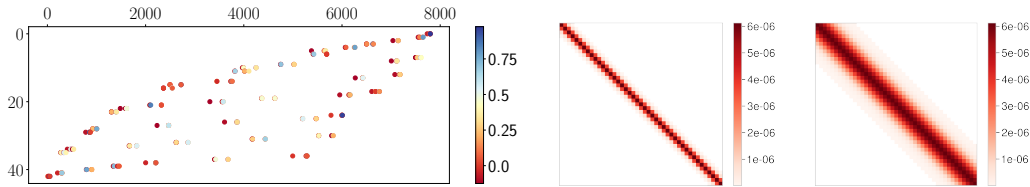


FIG. 4. Observation operator \mathcal{B}_k and observation error covariance matrix \mathbf{R}_k at any observation time instance t_k . To construct synthetic observation error covariances \mathbf{R}_k , we use a Gaspari–Cohn function (3.28) with a predefined length scale ℓ . Left: space observation operator \mathcal{B}_K . Middle: observation error covariance matrix \mathbf{R}_k with length scale of $\ell=1$. Right: observation error covariance matrix \mathbf{R}_k with length scale of $\ell=3$.

In the numerical experiments we use synthetic observations and consider two cases of observation correlations. First, we assume that observations are uncorrelated, with fixed standard deviation $\sigma_{\text{obs}} = 2.475 \times 10^{-2}$. This value is obtained by considering a noise level of 5% of the maximum

concentration of the contaminant at all observation points, found from a reference simulation, that is, the solution of (4.1), over the simulation timespan $[0, T]$, with the initial condition (Figure 3(right)). Second, we consider the case of space correlations where we run two sets of experiments with block diagonal covariance matrices, whose structure is shown in Figure 4. These are the covariances \mathbf{R}_k between observation gridpoints at any observation time t_k and are constructed by using the fifth-order piecewise-rational function (3.28), with covariance length scales $\ell = 1, \ell = 3$, respectively. We use (3.28) to create correlations $\rho_{i,j}$ between i and j entries of the correlation matrix and scale it by observation noise variance σ_{obs}^2 to create a spatial covariance model, as shown in Figure 4. The row/column ordering of the covariance matrix corresponds to the entries of an observation vector; see Figure 3(left). The spatial covariance is stationary and is fixed over time; that is, $\mathbf{R}_k = \mathbf{R}, \forall k$.

4.1.3. Forward and adjoint operators. The forward operator \mathbf{F} is evaluated by solving (4.1) over the simulation timespan, and the observation operator is applied to the solution to extract solution values at the sensor locations at the predefined observation time instances. We use a space-time formulation where the model states at all simulation time points are stacked in one vector. A forward operator $\mathbf{F}_{0,k} \equiv \mathbf{F}_{t_0 \rightarrow t_k}$ maps the discretized model parameter θ to the measurements at observational gridpoints at time instance t_k . If we define $\mathcal{S}_{0,k} \equiv \mathcal{S}_{t_0 \rightarrow t_k}$ to be the solution operator over the interval $[t_0, t_k]$, and since \mathcal{B}_k is the observation operator at time instance t_k , then $\mathbf{F}_{0,k}\theta = \mathcal{B}_k\mathcal{S}_{0,k}\theta$. In the experiments here, we use the same observational grid at all time instances; that is, $\mathcal{B}_k = \mathcal{B}, \forall k$. Note that \mathcal{B} here is an interpolation operator from the model gridpoints to observational gridpoints.

A space-time observation vector is defined as $\mathbf{y} = [\mathbf{y}_1^\top, \mathbf{y}_2^\top, \dots, \mathbf{y}_{n_t}^\top]^\top$, where $\mathbf{y}_k \equiv \mathbf{y}[t_k]$ represents the sensor measurements at time instance t_k , with entries ordered as shown in Figure 3(left). The observation error covariance matrix $\mathbf{\Gamma}_{\text{noise}}$ is defined accordingly (see Subsection 2.4 for more details). Given this space-time formulation, we can rewrite the forward problem (2.1) as

$$(4.2) \quad [\mathbf{y}_1^\top, \mathbf{y}_2^\top, \dots, \mathbf{y}_{n_t}^\top]^\top = \left[(\mathbf{F}_{0,1}\theta)^\top, (\mathbf{F}_{0,2}\theta)^\top, \dots, (\mathbf{F}_{0,n_t}\theta)^\top \right]^\top + \delta, \quad \delta \sim \mathcal{N}(\mathbf{0}, \mathbf{\Gamma}_{\text{noise}}).$$

When the observation noise is temporally uncorrelated, the observation error covariance matrix $\mathbf{\Gamma}_{\text{noise}}$ is block diagonal, and the forward model can be written in the form

$$(4.3) \quad \mathbf{y}_k = \mathbf{F}_{0,k}\theta + \delta_k, \quad \delta_k \sim \mathcal{N}(\mathbf{0}, \mathbf{R}_k), \quad k = 1, 2, \dots, n_t.$$

This formulation (4.3) of the forward problem is advantageous for large-scale time-dependent problems because *checkpointing* is essential for scalability of the solution of both the Bayesian inverse problem and the OED. Forward and adjoint simulations scale efficiently by checkpointing the model solution at observation time instances t_k and by utilizing a model solution operator $\mathcal{S}_{k-1,k} \equiv \mathcal{S}_{t_{k-1} \rightarrow t_k}$ to propagate the model state over the simulation window $[t_{k-1}, t_k]$.

For a linear operator \mathbf{F} , the adjoint \mathbf{F}^* satisfies the property $\langle \mathbf{F}\mathbf{x}, \mathbf{y} \rangle = \langle \mathbf{x}, \mathbf{F}^*\mathbf{y} \rangle$, where \mathbf{x}, \mathbf{y} are elements of the space on which the product is defined. If \mathbf{F} is defined on the Euclidean space equipped with inner product $\langle \mathbf{x}, \mathbf{y} \rangle := \mathbf{x}^\top \mathbf{y}$, then the adjoint of the forward operator is equal to the matrix transpose of the discretized forward operator; that is, $\mathbf{F}^* = \mathbf{F}^\top$. Here, however, we use a finite-element discretization of the linear Bayesian inverse problem where the underlying infinite-dimensional problem is formulated on the space equipped with $L^2(\mathcal{D})$ inner product. As explained in [14], the model adjoint is defined by using the Euclidean inner product weighted by the finite-element mass matrix \mathbf{M} . Specifically, for $\mathbf{u} \in \mathbb{R}^{N_\theta}$, $\mathbf{v} \in \mathbb{R}^{N_{\text{obs}}}$, it follows that $\langle \mathbf{F}\mathbf{u}, \mathbf{v} \rangle = (\mathbf{F}\mathbf{u})^\top \mathbf{v} =$

$\mathbf{u}^\top \mathbf{F}^\top \mathbf{v} = \mathbf{u}^\top \mathbf{M} \mathbf{M}^{-1} \mathbf{F}^\top \mathbf{v} = \langle \mathbf{u}, \mathbf{M}^{-1} \mathbf{F}^\top \mathbf{v} \rangle_{\mathbf{M}}$, resulting in the model adjoint $\mathbf{F}^* = \mathbf{M}^{-1} \mathbf{F}^\top$. In the time-dependent settings utilized here, the adjoint takes the form $\mathbf{F}_{k,0}^* = \mathbf{M}^{-1} \mathcal{S}_{0,k}^\top \mathcal{B}_k^\top$.

4.1.4. Goal operator and its adjoint. The QoI γ is the value of contaminant concentration predicted around the second building \mathbf{B}_2 (see [Figure 3](#)) at a future time instance t_p , beyond the simulation time. Specifically, we aim to predict the contaminant concentration withing a specific distance ϵ from the walls (i.e., boundary) of that building. For that, we set $\epsilon = 0.02$ and $t_p = 2.2$, which results in a prediction vector of size 138. If we define \mathbf{C}_p to be the matrix representation of a restriction operator that projects the solution at time t_p onto the prediction gridpoints (shown in [Figure 5](#)(left)), then the goal operator is defined as $\mathbf{P} = \mathbf{C}_p \mathcal{S}_{0,p}$. Since we are using finite-element discretization, the adjoint of the goal operator is defined as $\mathbf{P}^* = \mathbf{M}^{-1} \mathcal{S}_{0,p}^\top \mathbf{C}_p^\top$.

4.1.5. The prior. Following the setup in [\[6, 39\]](#), the prior distribution of the parameter θ is $\mathcal{N}(\theta_{\text{pr}}, \mathbf{\Gamma}_{\text{pr}})$, with $\mathbf{\Gamma}_{\text{pr}}$ being a discretization of \mathcal{A}^{-2} , where \mathcal{A} is a Laplacian operator. In particular, we use $\mathcal{A} = \delta I + \gamma \Theta \nabla$, where Θ is a symmetric positive definite tensor for anisotropic diffusion of the PDE [\(4.1\)](#), $\delta \gamma$ governs the variance of the prior samples, and the ratio $\frac{\gamma}{\delta}$ governs the correlation length scale [\[3, 50\]](#). In our experiments we set $\gamma = 1$ and $\delta = 16$. The ground truth and the prior QoI (shown in [Figure 5](#)(middle)) are obtained by applying the prediction operator \mathbf{P} to the true and the prior initial condition, respectively. That is, $\gamma_{\text{true}} = \mathbf{P} \theta_{\text{true}}$, and the goal QoI γ assumes a Gaussian prior $\mathcal{N}(\mathbf{P} \theta_{\text{pr}}, \mathbf{P} \mathbf{\Gamma}_{\text{pr}} \mathbf{P}^*)$. The prior covariance matrix of the goal QoI, that is, $\mathbf{P} \mathbf{\Gamma}_{\text{pr}} \mathbf{P}^*$, is displayed in [Figure 5](#)(right). The effect of the prior on the resulting design is an important issue; however, it is out of the scope of this work. Here we fix the prior across all experiments and focus on the performance due to observation covariance weighting.

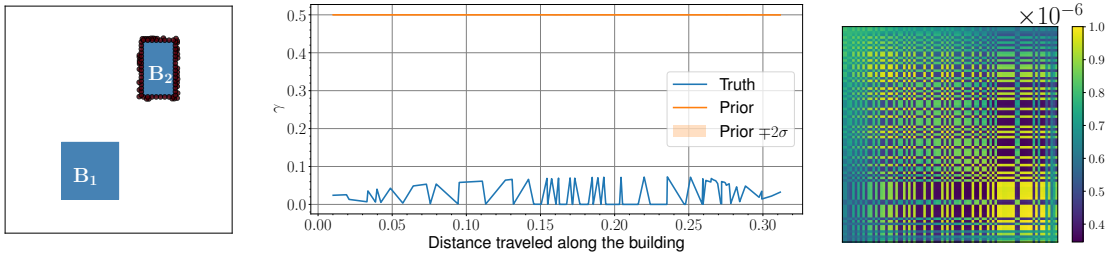


FIG. 5. *Left: gridpoints around the second building \mathbf{B}_2 , at which the goal QoI γ is predicted. Middle: ground truth and the prior of the goal QoI γ . Here, the x-axis of the middle panel corresponds to the prediction gridpoints shown in the left panel reordered based on the distance traveled along the second building starting from the lower-left corner. Right: entries of the prior covariance matrix $\mathbf{P} \mathbf{\Gamma}_{\text{pr}} \mathbf{P}^*$, with rows/columns reordered to match the ordering on the x-axis of [Figure 5](#)(middle).*

In the numerical results discussed in [Subsection 4.2](#), we use γ_{True} to calculate an accuracy measure of the solution of an inverse problem. Specifically, we use the root-mean-squared error (RMSE) of the QoI retrieved by Bayesian inversion γ defined as

$$(4.4) \quad \text{RMSE} := \frac{\|\gamma - \gamma_{\text{true}}\|_2}{\sqrt{N_{\text{goal}}}}.$$

4.1.6. OED regularization. We employ an ℓ_1 regularization term to induce a sparse design. Specifically, given the specific choice of the design weighting function ω , the regularization term and

the associated derivative take the form

$$(4.5) \quad \Phi(\zeta) = \|\omega(\zeta, \zeta)\|_1 = \sum_{i=1}^{n_s} |\omega(\zeta_i, \zeta_i)| = \sum_{i=1}^{n_s} \omega(\zeta_i, \zeta_i); \quad \nabla_{\zeta} \Phi(\zeta) = \sum_{i=1}^{n_t} \frac{\partial \omega(\zeta_i, \zeta_i)}{\partial \zeta_i} \mathbf{e}_i.$$

4.1.7. Optimization algorithms. To solve the OED problem (2.8), we use Python’s optimization routines provided in Scipy. Specifically, we use the implementation of L-BFGS-B [15, 46], provided by `fmin_l_bfgs_b()` with a stopping criterion based on the maximum entry of the projected gradient. We set the tolerance to `pgtol = 1 × 10-5`. This allows us to set bound constraints when needed, for example, when the kernel (3.12) is invoked. For all choices of the weighting function, the initial guess passed to the optimization algorithm is set to yield weighting values $\omega(\zeta_i, \zeta_i) = 0.5$; $i = 1, 2, \dots, n_s$. This means that all sensors are as likely to be activated as to be turned off.

4.2. Numerical results. We investigate several scenarios. The first case is where no observation correlations are considered; then we incorporate spatial correlations. The correlations are synthetically generated by using a Gaspari–Cohn function with a predefined length scale. Note that this choice is made for convenience to create synthetic covariances and is independent from the weighting function ρ used to control the temporal relative importance of observation covariances; see Subsection 3.6. We use A-optimality as the main criterion for sensor placement in our numerical experiments. As discussed in Section 3, we can use a randomized trace estimator to formulate the optimality criterion and the associated gradient. In our experiments we used the Hutchinson randomized trace estimator to approximate the A-optimality criterion, and we set the sample size to $n_r = 25$. This enabled us to carry out several comparative experiments both accurately and efficiently. Numerical results validating this assertion are given in Appendix D.2. For fair comparison, we used the same realizations of random vectors to calculate the objective, namely, the optimality criterion, and the gradients in all experiments.

Note that while the A-optimality criterion is calculated based on the sum of the posterior variances discarding posterior covariances, it does in fact account for observation correlations, since posterior variances are influenced by both prior and observation error covariances (see (2.3)). Since the case with temporal observation correlations is not applicable here and since D-optimality might be more suitable for handling spatiotemporal observation correlations, we will leave the investigation of this case to future studies.

We are interested mainly in the design of an observational grid that will optimally serve the Bayesian retrieval of the goal QoI. Specifically, we are looking for the optimal subset of candidate sensor locations to deploy for data collection. We start by showing the results of solving the Bayesian inverse problem, with a fully deployed observational grid. Figure 6 shows the ground truth, the prior, and the posterior prediction QoI γ obtained by solving the Bayesian inverse problem with all sensors activated. The results are shown for the case where no observation correlations are assumed, that is, when the correlation length scale is $\ell = 0$, and two experiments with space correlations with ℓ set to 1 and 3, respectively. This plot will serve as a visual benchmark as needed.

The goal of solving an OED problem is to find a small subset of sensors (e.g., given a limited budget) that yields a posterior QoI as close as possible to the ground truth shown in Figure 5(right), with minimum uncertainty. In what follows, we assume a maximum budget of λ observation sensors to be ideally placed in the domain. The solution of the OED problem is expected to be sparse but might not be binary. A simple rounding method to obtain a binary design is used when needed, by

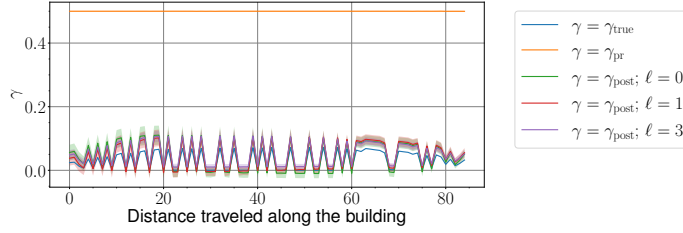


FIG. 6. The truth, the prior, and the posterior ($\pm 2\sigma_{\text{post}}$) prediction QoI γ . The truth is based on the ground truth of the model initial condition. The prior QoI is based on the mean of the prior distribution for all scenarios. The posterior prediction QoI is obtained by using the solution of the inverse problem, using all candidate sensors. The correlation length scale used in the Gaspari–Cohn function to construct correlations is indicated in the legends. The case when $\ell = 0$ corresponds to the diagonal covariance matrix, that is, no correlations, is assumed.

activating the sensors corresponding to the largest λ weights in the design resulting from solving an OED optimization problem. In our experiments we show results for two choices of the budget λ : first $\lambda = 8$ and second $\lambda = n_s/2$, where we allow up to 50% of the sensors to be activated. We discuss results obtained by solving the OED problem (2.8) with the A-optimality criterion $\Psi(\zeta) = \Psi^{\text{GA}}$, using the product kernel (3.12), the EXP kernel (3.13), and the logistic sigmoid (3.14) kernels. Experiments are carried out for multiple values of the regularization parameter α , to study the effect of the regularization term on both sparsity and the order of relative importance of candidate sensors. We start with numerical experiments with uncorrelated observation errors, and then we show experiments with spatial observation correlations with multiple length scales, as described in Section 4.

4.2.1. No-correlations results. Figure 7 shows the optimal weights resulting from solving the standard OED relaxation (2.8) with ad hoc fix (3.1) and the OED problem using the Schur-product formulation (3.16a) with the weighting matrix $\mathbf{W}(\zeta)$ defined using the kernel (3.12), the EXP kernel (3.13), and the logistic sigmoid kernels (3.14), respectively, for multiple values of the penalty parameter α . All formulations behave similarly and yield similar estimates of the optimal design. Note that in this setup the sigmoid weighting kernel (3.14) leads to a sparser design even with a penalty value $\alpha = 0$, that is, without enforcing a sparsity-promoting penalty term.

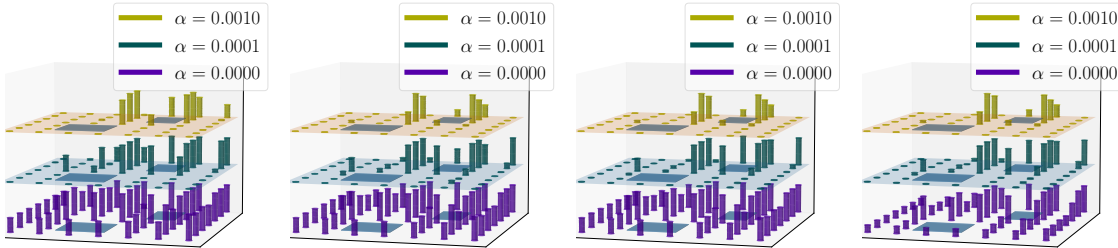


FIG. 7. Optimal weights resulting from solving the OED problem (2.8). Results are obtained (from left to right) by using the standard OED formalism (2.8) with ad hoc fix (3.1), Schur-OED with weighting kernel (3.12), the EXP kernel (3.13), and the logistic sigmoid kernels (3.14), respectively, for values of the parameter α set to 0, $1e-4$, $1e-3$. The solution is plotted in the form of bars located on the grid at the corresponding candidate sensor locations. The height of each bar is set to the value of the weight obtained by solving (2.8). The z -axis has a scale (limits) set to $[0, 1]$ for all subplots to fairly compare the values of weights resulting by solving the relaxed OED problem.

To better inspect the difference between the resulting optimal designs shown in Figure 7, we apply rounding to obtain a binary design by activating the maximum $\lambda = 8$ sensors; the resulting

binary designs are shown in Figure 8. The results in Figure 7 and Figure 8 indicate that, in general,

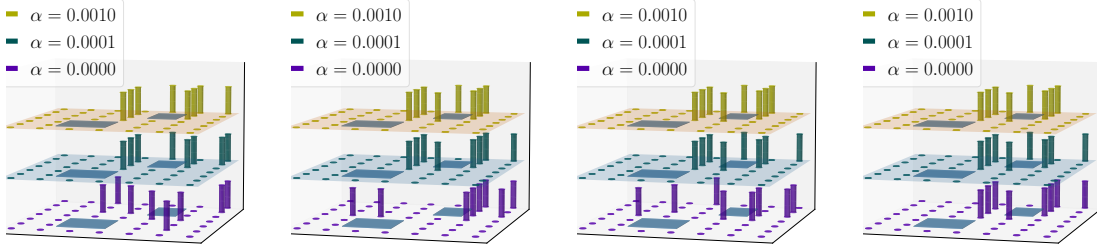


FIG. 8. Similar to Figure 7. Here we show the binary design corresponding to the highest $\lambda = 8$ weights.

increasing the value of the penalty parameter enforces sparsification on the solution of the OED problem. However, the optimal weights, the ranking, and the sparsity levels obtained by the four kernels are not identical. It would be hard, however, to judge which solution is better without inspecting two elements: the trace of the posterior covariance (i.e., the OED optimality criterion) and the quality of the solution of an inverse problem obtained by reconfiguring the observational grid based on the optimal weights obtained.

To be able to fairly judge the quality of the A-optimal designs, we inspect the value of the optimality criterion corresponding to the optimal solution. Table 1 shows the value of the A-optimality criterion, namely, the trace of the posterior covariance matrix, obtained by the optimal design before and after thresholding for multiple values of the penalty parameter α . Results are obtained (from left to right) by using the standard OED formalism (2.8) with ad hoc fix (3.1), and the Schur-OED formulation (3.16a) with the weighting matrix $\mathbf{W}(\zeta)$ defined using the kernel (3.12), the EXP kernel (3.13), and the logistic sigmoid kernels (3.14), respectively. For each choice of the weighting kernel, the first column shows the value of the posterior covariance trace obtained by setting the design to the solution of the relaxed OED problem (2.8), that is, $\Psi^{\text{GA}}(\zeta) = \text{Tr}(\Sigma_{\text{post}}(\zeta))$ with $\zeta = \zeta^{\text{opt}}$. The results in the second column correspond to the value of the optimality criterion $\Psi^{\text{GA}}(\zeta^{\text{b}})$, where ζ^{b} is a binary design obtained by setting the entries of ζ^{opt} corresponding to the highest $\lambda = 8$ weights to 1 and everything else to zero. The third column is similar to the second column, but the binary design is obtained by activating the sensors corresponding to the highest $n_{\text{s}}/2$ weights. The results of both the standard and the Schur-product OED formulations are almost identical, with similar estimates of the optimal design.

TABLE 1

Value of the A-optimality criterion, namely, the trace of the posterior covariance matrix $\Psi^{\text{GA}}(\zeta) = \text{Tr}(\Sigma_{\text{post}}(\zeta))$, multiplied by 10^3 , obtained by the optimal design, before and after thresholding, for multiple values of the penalty parameter. Here, observations are assumed to be uncorrelated. Two thresholding/rounding approaches are used: (1) “Max 8,” in which the $\lambda = 8$ sensors with highest weights are activated, and (2) “Median,” in which all sensors with weights above the median value of the optimal weights are activated.

| Regularization Penalty | Standard OED (2.8, 3.1) | | | Product Kernel (3.12) | | | EXP Kernel (3.13) | | | Sigmoid Kernel (3.14) | | |
|------------------------|-------------------------|--------------------|--------|-----------------------|--------------------|--------|-------------------|--------------------|--------|-----------------------|--------------------|--------|
| | A-optimal Design | Thresholded Design | | A-optimal Design | Thresholded Design | | A-optimal Design | Thresholded Design | | A-optimal Design | Thresholded Design | |
| | | Max 8 | Median | | Max 8 | Median | | Max 8 | Median | | Max 8 | Median |
| $\alpha = 0$ | 8.960 | 14.390 | 9.390 | 8.960 | 45.890 | 9.40 | 8.960 | 45.890 | 9.40 | 9.060 | 10.520 | 9.40 |
| $\alpha = 1e - 4$ | 9.240 | 13.860 | 9.460 | 9.360 | 10.520 | 9.420 | 9.350 | 10.460 | 9.40 | 9.390 | 10.460 | 9.40 |
| $\alpha = 3e - 4$ | 9.640 | 11.130 | 9.480 | 9.880 | 10.390 | 9.480 | 9.920 | 10.480 | 9.40 | 9.910 | 10.480 | 9.480 |
| $\alpha = 5e - 4$ | 10.010 | 11.130 | 9.850 | 10.290 | 10.480 | 9.480 | 10.30 | 10.480 | 9.40 | 10.350 | 10.480 | 9.40 |
| $\alpha = 1e - 3$ | 10.690 | 11.130 | 9.890 | 11.250 | 10.480 | 9.650 | 11.250 | 10.480 | 9.530 | 11.260 | 10.480 | 9.480 |

Now we turn our attention to the quality of the solution of an inverse problem (MAP point) obtained by reconfiguring the observational grid based on the optimal design. First, the observational

grid is reconfigured as follows. We solve the A-OED problem to obtain the optimal design vector ζ^{opt} ; and then we calculate the vector of optimal weights $\varpi(\zeta^{\text{opt}}, \zeta^{\text{opt}})$, which is then rounded to yield a binary design ζ^{b} . The resulting binary design ζ^{b} is used to reconfigure the observation grid, the observation operator—hence the forward operator \mathbf{F} —and the observation error covariance matrix. The inverse problem is then solved by using the reconfigured settings. Table 2 shows the RMSE results obtained by solving the inverse problem using the binary designs corresponding to optimal designs with objective values shown in Table 1. We also show the RMSE results corresponding to the prior QoI and the solution of the inverse problem with all sensors activated, setting a benchmark of the RMSE values. The four settings yield optimal (rounded) designs that result in high-quality solutions of the inverse problems as suggested by the small RMSE values. These results are also supported by the results in Figure 9, which displays the solution of the inverse problem along with the associated posterior uncertainties. Thus, in the case of uncorrelated observational errors, both the standard (pre- and postmultiplication of the precision matrix with the relaxed design) and the Schur-OED formalism behave almost identically except that the Schur-OED optimization problem with logistic kernel is solved without enforcing bound constraints on the design. Note that by allowing more sensors to be deployed, additional data is collected, and hence more information is gained. This is supported by the decrease in both objective values (Table 1) and the RMSE results (Table 2) when the number of sensors is increased from “Max 8” to “Median” rounding.

TABLE 2

Similar to Table 1. Here we show the RMSE results obtained by solving the inverse problem given the optimal design.

| Regularization Penalty | RMSE | | | | | | | | | |
|------------------------|-------------|-----------|-------------------------|---------|-----------------------|---------|-------------------|---------|-----------------------|---------|
| | All Sensors | | Standard OED (2.8, 3.1) | | Product Kernel (3.12) | | EXP Kernel (3.13) | | Sigmoid Kernel (3.14) | |
| | Prior | Posterior | Max 8 | Median | Max 8 | Median | Max 8 | Median | Max 8 | Median |
| $\alpha = 0$ | 0.4704 | 0.0258 | 0.02751 | 0.02610 | 0.05295 | 0.02798 | 0.05295 | 0.02798 | 0.04048 | 0.02799 |
| $\alpha = 1e-4$ | | | 0.04154 | 0.02717 | 0.04048 | 0.02724 | 0.03984 | 0.02714 | 0.03984 | 0.02714 |
| $\alpha = 3e-4$ | | | 0.03966 | 0.02805 | 0.03190 | 0.02971 | 0.04040 | 0.02797 | 0.04040 | 0.02971 |
| $\alpha = 5e-4$ | | | 0.03966 | 0.03352 | 0.04040 | 0.02967 | 0.04040 | 0.02797 | 0.04040 | 0.02797 |
| $\alpha = 1e-3$ | | | 0.03966 | 0.03364 | 0.04040 | 0.03136 | 0.04040 | 0.03028 | 0.04040 | 0.02971 |

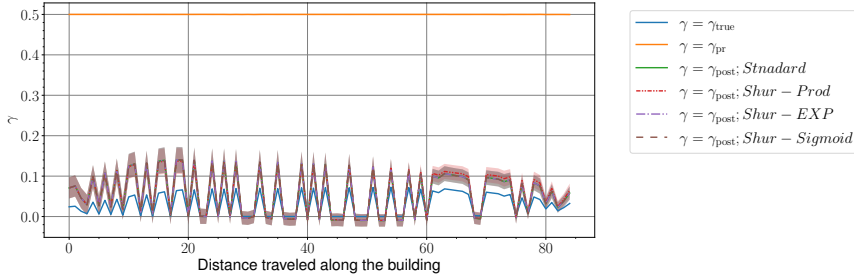


FIG. 9. Solution of the inverse problem, along with associated uncertainty ($\pm 2\sigma_{\text{post}}$), obtained based on the rounded A-optimal design resulting from solving the OED problem using settings described in Figure 7. Here, observations are assumed to be uncorrelated, and we show results obtained with $\alpha = 1e-4$ and with $\lambda = 8$ sensors activated. Inversion results here correspond to the second row of results in Table 2.

4.2.2. Space-correlations results. Here we show the results of experiments carried out with spatially correlated observations. Figure 10 shows the rounded binary designs obtained by setting the correlation length scale to $\ell = 1$, and Figure 11 shows binary designs for $\ell = 3$. Similar to the discussion in Subsection 4.2.1, results are shown here for multiple values of the penalty parameter α . These results (in comparison with Figure 8) indicate that discarding the observation correlations in an OED problem results in different optimal designs and thus can greatly degrade the quality of the

solution of an inverse problem. Moreover, in the presence of spatial correlations between neighboring candidate sensor locations, the optimal design tends to be more spread in the domain.

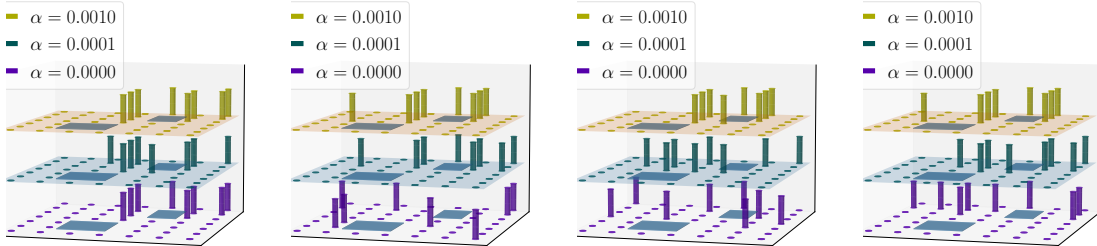


FIG. 10. Similar to Figure 8. Here we allow observation correlations with length scale $\ell = 1$.

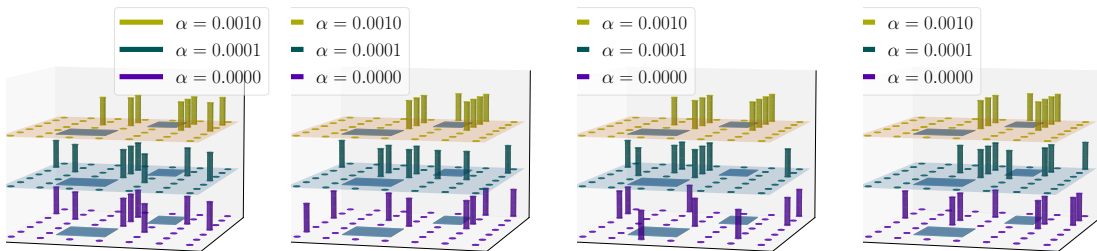


FIG. 11. Similar to Figure 8. Here we allow observation correlations with length scale $\ell = 3$.

To understand the empirical performance of the experiments carried out with observation spatial correlations, we analyze the value of the optimality criterion (Table 3) as well as the RMSE results (Table 4). Table 3 shows the value of the A-optimality criterion, namely, the trace of the posterior covariance matrix, obtained by the optimal design, before and after thresholding, for multiple values of the penalty parameter α . The results in Table 3 show that the standard OED formulation is not consistent with the Schur-OED formulation. It is hard to compare the two sets of results because they show numerical approximation obtained by using two different objective functions. Nevertheless, this comparison can in part be made based on the accuracy of the resulting solution, for example, by inspecting RMSE results. Table 4 shows the RMSE of the solution of the inverse problem corresponding to optimal designs with objective values displayed in Table 3. The overall performance explained by results in Table 4 shows that the Schur-OED formulation outperforms the standard OED formulation especially for stronger presence of observational error correlations, for example, for larger correlation length scale. We note that with a wider correlation length scale, that is, by allowing more sensors to be highly correlated, fewer sensors are required to achieve high accuracy. This is explained by the significant drop in RMSE values from $\ell = 1$ to $\ell = 3$. This is also obvious by comparing the RMSE results in Table 4 with Table 2.

We conclude this section by showing the solution of the inverse problem obtained by reconfiguring the observational setup based on the A-optimal design resulting from (2.8) in the presence of observation correlations; see Figure 12. These results support our assertion that with increasing correlation length scale, fewer sensors are needed achieve high levels of accuracy. The results also show that the Schur-OED formulation outperforms the standard OED approach especially for larger correlation length scales.

TABLE 3

Similar to Table 1. Here we allow observation correlations, with correlation length scale ℓ set to $\ell = 1$ and $\ell = 3$, respectively.

| Correlation Length-scale | Regularization Penalty | Standard OED (2.8, 3.1) | | | Product Kernel (3.12) | | | EXP Kernel (3.13) | | | Sigmoid Kernel (3.14) | | |
|--------------------------|------------------------|-------------------------|--------------------|--------|-----------------------|--------------------|--------|-------------------|--------------------|--------|-----------------------|--------------------|--------|
| | | A-optimal | Thresholded Design | | A-optimal | Thresholded Design | | A-optimal | Thresholded Design | | A-optimal | Thresholded Design | |
| | | Design | Max 8 | Median | Design | Max 8 | Median | Design | Max 8 | Median | Design | Max 8 | Median |
| $\ell = 1$ | $\alpha = 0$ | 6.790 | 7.790 | 7.110 | 7.010 | 27.770 | 7.190 | 7.010 | 29.620 | 7.180 | 7.040 | 89.830 | 8.280 |
| | $\alpha = 1e-4$ | 6.830 | 7.750 | 7.030 | 8.120 | 9.380 | 7.320 | 8.080 | 18.250 | 7.190 | 8.150 | 10.420 | 7.360 |
| | $\alpha = 3e-4$ | 7.240 | 8.570 | 7.280 | 9.080 | 7.660 | 7.220 | 8.750 | 8.310 | 7.250 | 9.020 | 7.090 | 7.130 |
| | $\alpha = 5e-4$ | 7.620 | 7.790 | 7.190 | 9.610 | 7.660 | 7.220 | 9.690 | 7.810 | 7.270 | 10.170 | 7.770 | 7.050 |
| | $\alpha = 1e-3$ | 7.90 | 7.790 | 7.390 | 11.230 | 7.250 | 6.760 | 11.220 | 7.280 | 6.940 | 11.230 | 7.250 | 6.680 |
| $\ell = 3$ | $\alpha = 0$ | 3.290 | 5.810 | 3.210 | 3.360 | 32.410 | 2.330 | 3.530 | 43.410 | 2.290 | 3.290 | 6.470 | 2.890 |
| | $\alpha = 1e-4$ | 3.290 | 5.810 | 3.210 | 4.990 | 21.170 | 2.470 | 4.310 | 8.350 | 2.30 | 7.650 | 3.860 | 2.410 |
| | $\alpha = 3e-4$ | 3.30 | 5.810 | 3.210 | 6.530 | 3.990 | 2.870 | 6.310 | 3.990 | 2.630 | 7.450 | 3.260 | 2.550 |
| | $\alpha = 5e-4$ | 3.040 | 3.450 | 2.550 | 7.320 | 3.640 | 2.690 | 6.880 | 3.710 | 2.60 | 9.20 | 3.870 | 2.340 |
| | $\alpha = 1e-3$ | 3.640 | 3.390 | 2.90 | 10.690 | 3.730 | 2.260 | 6.520 | 3.310 | 2.410 | 10.650 | 3.730 | 2.160 |

TABLE 4

Similar to Table 2. Here we allow observation correlations, with correlation length scale ℓ set to $\ell = 1$ and $\ell = 3$, respectively.

| Correlation Length-scale | Regularization Penalty | RMSE | | | | | | | | | |
|--------------------------|------------------------|-------------|-----------|-------------------------|---------|-----------------------|---------|-------------------|---------|-----------------------|---------|
| | | All Sensors | | Standard OED (2.8, 3.1) | | Product Kernel (3.12) | | EXP Kernel (3.13) | | Sigmoid Kernel (3.14) | |
| | | Prior | Posterior | Max 8 | Median | Max 8 | Median | Max 8 | Median | Max 8 | Median |
| $\ell = 1$ | $\alpha = 0$ | 0.4704 | 0.0225 | 0.04457 | 0.01799 | 0.05667 | 0.02262 | 0.02969 | 0.02249 | 0.08218 | 0.02327 |
| | $\alpha = 1e-4$ | | | 0.05227 | 0.02434 | 0.02036 | 0.01358 | 0.01594 | 0.01315 | 0.05219 | 0.01491 |
| | $\alpha = 3e-4$ | | | 0.04535 | 0.02130 | 0.02321 | 0.01960 | 0.02374 | 0.01401 | 0.04955 | 0.02212 |
| | $\alpha = 5e-4$ | | | 0.04457 | 0.03283 | 0.02321 | 0.01960 | 0.02417 | 0.01919 | 0.04694 | 0.02998 |
| | $\alpha = 1e-3$ | | | 0.04457 | 0.01959 | 0.03310 | 0.03169 | 0.05018 | 0.02870 | 0.03310 | 0.03056 |
| $\ell = 3$ | $\alpha = 0$ | 0.4704 | 0.0239 | 0.05055 | 0.02920 | 0.08058 | 0.01356 | 0.10616 | 0.01053 | 0.02389 | 0.02499 |
| | $\alpha = 1e-4$ | | | 0.05055 | 0.02920 | 0.14247 | 0.01687 | 0.01879 | 0.00903 | 0.01820 | 0.01177 |
| | $\alpha = 3e-4$ | | | 0.05055 | 0.02920 | 0.01711 | 0.01880 | 0.01711 | 0.02025 | 0.01820 | 0.01177 |
| | $\alpha = 5e-4$ | | | 0.04985 | 0.01161 | 0.02042 | 0.01892 | 0.01832 | 0.01337 | 0.01179 | 0.01152 |
| | $\alpha = 1e-3$ | | | 0.04763 | 0.02041 | 0.04279 | 0.01124 | 0.02722 | 0.00988 | 0.01279 | 0.00755 |

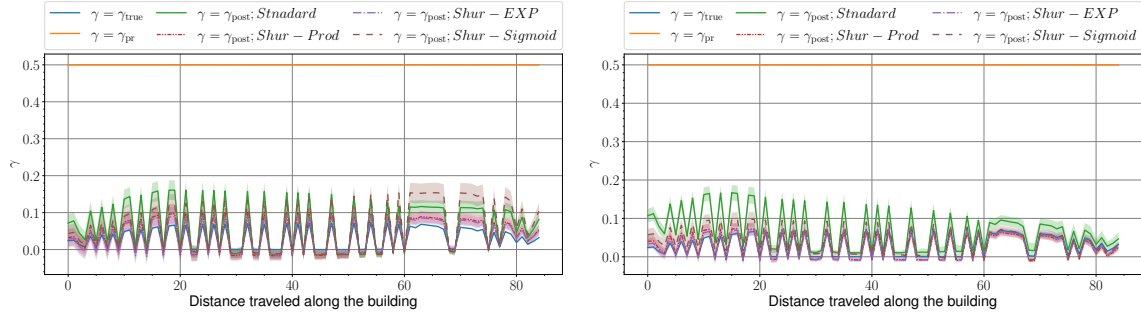


FIG. 12. Similar to Figure 9. Here, observations are assumed to be correlated with length scale ℓ , with $\ell = 1$ (left), and with $\ell = 3$ (right), respectively. We show results obtained with $\alpha = 1e-4$, and $\lambda = 8$ sensors are activated.

The numerical results presented in this section reveal that solving an OED problem for sensor placement before carrying out Bayesian inversion is an essential step to guarantee an optimal deployment of observational grid under a limited budget. While the traditional formulation of the OED problem is useful, its performance can be enhanced by employing the generalized formulation suggested in this work, especially in the presence of observation correlations. Specifically, while it can be tempting for simplicity to ignore observation correlations in the process of solving an OED problem, one will likely end up with a suboptimal design that can lead to erroneous solution of the inverse problem.

5. Conclusion. In this work we presented a generalized approach for optimal experimental design for linear Bayesian inverse problems where the measurement errors are generally correlated. This study supplements the fast-evolving literature on OED for the Bayesian inverse problem; it provides an extended mathematical formulation of the most popular optimality criteria, as well as the associated gradients, essential for the numerical solution of the optimization problem. The

proposed formulation follows a Hadamard product approach to formulate the weighted likelihood, which is then used in the optimality criterion. This approach provides a clear understanding of the effect of the design on the measurements and the covariances of observational errors and is valid in both finite- and infinite-dimensional settings of Bayesian linear inverse problems. We show that the traditional formulation of the OED problem is a special case of the proposed approach in the case of uncorrelated observations, where the observation precision matrix is weighted by the relaxed design. The Hadamard product formulation is shown to be accurate and more flexible, especially for handling spatiotemporal correlations. We provide multiple candidates of the weighting function that evaluates the relative importance of observation covariances. Our numerical results show that the proposed formulation achieves better results than by using the traditional formulation, that is, by pre- and postmultiplication of the observation error precision matrix with the relaxed design. All weighting functions investigated here achieved similar performance in the presence of observation correlations with larger length scale, that is, by allowing more sensors to be correlated. By using a logistic sigmoid function for covariance weighting, however, the OED optimization problem transforms into an unconstrained optimization problem, which is generally easier to solve than the traditional OED problem with box constraints.

The main limitation of the proposed approach is the requirement of differentiability of the regularization term. In this work we follow the common practice of approximating the sparsification-enforcing penalty ℓ_0 with a penalty function based on ℓ_1 norm, which is differentiable given that the weights fall in the interval $[0, 1]$. A recent approach that does not require differentiability of the objective function with respect to the design, and thus enables sparsification penalties such as ℓ_0 , is proposed in [8]. However, this approach does not apply any relaxation to the design variables and is thus out of the scope of this work.

While we provided the mathematical formulation of the approach for A- and D-optimal designs, we focused our numerical experiments on A-optimality in the presence of spatial correlations. Extensions of the mathematical formulation and empirical studies of D-optimal designs in the presence of correlations in space and time domains are still required. Algorithmic approaches such as the standard greedy swapping (exchange) algorithm [21, 37, 52] can be used to seek a local optimum of the OED objective; however, as with the coordinate descent optimization approach, it can be computationally expensive for increasing cardinality of the design space. This work focused on extending the popular relaxation approach for solving binary OED formulation where gradient-based optimization routines are utilized to find a local minimum of the OED objective. Nevertheless, in future work we plan to provide empirical comparisons to assess the quality and computational cost of various OED formulations and solution approaches.

Appendix A. Proofs of Theorems and Lemmas Discussed in Section 3.

Proof of Lemma 3.1. Let $\mathbf{A} := \mathbf{W}\Gamma_{\text{noise}}\mathbf{W}^T$ and $\mathbf{A}^\dagger := \mathbf{L}^T (\mathbf{L}\mathbf{W}\Gamma_{\text{noise}}\mathbf{W}^T\mathbf{L}^T)^{-1} \mathbf{L}$, where we dropped the dependency of \mathbf{L} and \mathbf{W} for clarity. By the definition of \mathbf{L} and \mathbf{W} , it follows that $\mathbf{L}^T\mathbf{L}\mathbf{W} = \mathbf{W} = \mathbf{W}^T = \mathbf{W}^T\mathbf{L}^T\mathbf{L}$, and hence the following hold:

- i $\mathbf{A}\mathbf{A}^\dagger = \mathbf{L}^T\mathbf{L}\mathbf{W}\Gamma_{\text{noise}}\mathbf{W}^T\mathbf{L}^T (\mathbf{L}\mathbf{W}\Gamma_{\text{noise}}\mathbf{W}^T\mathbf{L}^T)^{-1} \mathbf{L} = \mathbf{L}^T\mathbf{L}$.
- ii $\mathbf{A}^\dagger\mathbf{A} = \mathbf{L}^T (\mathbf{L}\mathbf{W}\Gamma_{\text{noise}}\mathbf{W}^T\mathbf{L}^T)^{-1} \mathbf{L}\mathbf{W}\Gamma_{\text{noise}}\mathbf{W}^T\mathbf{L}^T\mathbf{L} = \mathbf{L}^T\mathbf{L}$.

It follows from (i), (ii) that the four conditions of a pseudo inverse matrix are then satisfied:

1. $\mathbf{A}\mathbf{A}^\dagger\mathbf{A} = \mathbf{L}^T\mathbf{L}\mathbf{A} = \mathbf{L}^T\mathbf{L}\mathbf{W}\Gamma_{\text{noise}}\mathbf{W}^T = \mathbf{W}\Gamma_{\text{noise}}\mathbf{W}^T = \mathbf{A}$.
2. $\mathbf{A}^\dagger\mathbf{A}\mathbf{A}^\dagger = \mathbf{L}^T\mathbf{L}\mathbf{A}^\dagger = \mathbf{L}^T\mathbf{L}\mathbf{L}^T (\mathbf{L}\mathbf{W}\Gamma_{\text{noise}}\mathbf{W}^T\mathbf{L}^T)^{-1} \mathbf{L} = \mathbf{L}^T (\mathbf{L}\mathbf{W}\Gamma_{\text{noise}}\mathbf{W}^T\mathbf{L}^T)^{-1} \mathbf{L} = \mathbf{A}^\dagger$,

where we used the fact that $\mathbf{L}\mathbf{L}^\top = \mathbf{I}$, the identity matrix.

$$3. (\mathbf{A}\mathbf{A}^\dagger)^\top = (\mathbf{L}^\top\mathbf{L})^\top = \mathbf{L}^\top\mathbf{L} = \mathbf{A}\mathbf{A}^\dagger.$$

$$4. (\mathbf{A}^\dagger\mathbf{A})^\top = (\mathbf{L}^\top\mathbf{L})^\top = \mathbf{L}^\top\mathbf{L} = \mathbf{A}^\dagger\mathbf{A} . \quad \square$$

Proof of Lemma 3.2. The proof follows easily by noting that

$$\mathbf{L}^\top(\zeta)\mathbf{L}(\zeta) (\mathbf{W}(\zeta) \odot \mathbf{\Gamma}_{\text{noise}}) = \mathbf{W}(\zeta) \odot \mathbf{\Gamma}_{\text{noise}} = (\mathbf{W}(\zeta) \odot \mathbf{\Gamma}_{\text{noise}}) \mathbf{L}^\top(\zeta)\mathbf{L}(\zeta),$$

and by following the same steps in the proof of Lemma 3.1. \square

Proof of Lemma 3.3. By definition of \mathbf{W} , if $\zeta \rightarrow \mathbf{1}$, then $\mathbf{W} \rightarrow \mathbf{1}$ and thus $\mathbf{W}_\Gamma \odot \mathbf{\Gamma}_{\text{noise}} \rightarrow \mathbf{\Gamma}_{\text{noise}}$, and $(\mathbf{W}_\Gamma \odot \mathbf{\Gamma}_{\text{noise}})^{-1} \rightarrow \mathbf{\Gamma}_{\text{noise}}^{-1}$, which proves the first part of the statement. To prove the statement for $\zeta \rightarrow \mathbf{0}$, by letting $\mathbf{s} := \text{diag}(\mathbf{\Gamma}_{\text{noise}})$, and $\mathbf{d}(\zeta) := (d_1(\zeta_1), \dots, d_{n_s}(\zeta_{n_s}))$ with

$$d_i(\zeta_i) := \begin{cases} 0; & \zeta_i = 0 \\ \frac{1-\zeta_i^4}{\zeta_i^2}; & \zeta_i \neq 0, \end{cases}$$

one can show that

$$(A.1) \quad \mathbf{W}(\zeta) \odot \mathbf{\Gamma}_{\text{noise}} = \text{Diag}(\mathbf{s} \odot \mathbf{d}(\zeta)) + \text{Diag}(\zeta) \mathbf{\Gamma}_{\text{noise}} \text{Diag}(\zeta) .$$

Since the second term of the right hand side of (A.1) is positive semi-definite, by employing Löwner ordering [32, 42], it follows that

$$(A.2) \quad \mathbf{W}(\zeta) \odot \mathbf{\Gamma}_{\text{noise}} \succeq \text{Diag}(\mathbf{s} \odot \mathbf{d}(\zeta)) ,$$

which implies

$$(A.3) \quad (\mathbf{W}(\zeta) \odot \mathbf{\Gamma}_{\text{noise}})^{-1} \preceq (\text{Diag}(\mathbf{s} \odot \mathbf{d}(\zeta)))^{-1} .$$

Since the trace preserves the Löwner ordering, it follows that

$$(A.4) \quad 0 \leq \text{Tr}\left((\mathbf{W}(\zeta) \odot \mathbf{\Gamma}_{\text{noise}})^{-1}\right) \leq \text{Tr}\left((\text{Diag}(\mathbf{s} \odot \mathbf{d}(\zeta)))^{-1}\right) = \sum_{i=1}^{n_s} \frac{\zeta_i^2}{1-\zeta_i^4} \cdot \frac{1}{(\mathbf{\Gamma}_{\text{noise}})_{ii}} .$$

By letting $\zeta \rightarrow \mathbf{0}$ it follows that $\text{Tr}\left((\mathbf{W}(\zeta) \odot \mathbf{\Gamma}_{\text{noise}})^{-1}\right) \rightarrow 0$ and hence $(\mathbf{W}(\zeta) \odot \mathbf{\Gamma}_{\text{noise}})^{-1} \rightarrow \mathbf{0}$ which immediately yields the desired conclusion. \square

Proof of Theorem 3.4. We consider three possible cases. First, if $\zeta \rightarrow \mathbf{1}$, $w_i \rightarrow 1$ for all $i = 1, \dots, n_s$, then $\mathbf{W}(\zeta) \rightarrow \mathbf{1}$ and $\mathbf{W}_\Gamma(\zeta) = (\mathbf{W}(\zeta) \odot \mathbf{\Gamma}_{\text{noise}})^{-1} \rightarrow \mathbf{\Gamma}_{\text{noise}}^{-1}$, resembling the case of activating all sensors. This also follows immediately from Lemma 3.3. Second, if $\zeta \rightarrow \mathbf{0}$, then $w_{i,j} = \zeta_i \zeta_j \rightarrow 0$, and $\frac{1}{w_{i,i}} = \frac{1}{\zeta_i^2} \rightarrow \infty$. From Lemma 3.3 it follows in this case that $(\mathbf{W}(\zeta) \odot \mathbf{\Gamma}_{\text{noise}})^\dagger \rightarrow \mathbf{0}$, which properly represents the case of disabling all sensors.

Third, we study the case where $\zeta \rightarrow \zeta^b$ where ζ^b is a boundary point other than $\mathbf{0}$ or $\mathbf{1}$. Let the observation covariance matrix $\mathbf{\Gamma}_{\text{noise}}$ and the weighting matrix \mathbf{W} be represented as block matrices as follows:

$$(A.5) \quad \mathbf{\Gamma}_{\text{noise}} = \begin{bmatrix} \mathbf{A} & \mathbf{B} \\ \mathbf{B}^\top & \mathbf{D} \end{bmatrix}; \quad \mathbf{W} = \begin{bmatrix} \mathbf{W}_A & \mathbf{W}_B \\ \mathbf{W}_B^\top & \mathbf{W}_D \end{bmatrix} .$$

Without loss of generality, we assume that both \mathbf{A} , \mathbf{W}_A correspond to elements of ζ^b that are equal to 0; permutation can be used to reach this form. In this case,

$$(A.6) \quad (\mathbf{\Gamma}_{\text{noise}} \odot \mathbf{W}(\zeta^b))^\dagger = \begin{bmatrix} \mathbf{0} & \mathbf{0} \\ \mathbf{0} & \mathbf{D}^{-1} \end{bmatrix}.$$

Note that the weighted precision matrix $\mathbf{W}_\Gamma(\zeta) = (\mathbf{W}(\zeta) \odot \mathbf{\Gamma}_{\text{noise}})^{-1}$ for $\zeta \in (0, 1)^{n_s}$, that is, for designs in the interior of the design variable domain. Thus, we write the precision matrix using block inversion as follows

$$(A.7) \quad \begin{aligned} \mathbf{W}_\Gamma(\zeta) &= (\mathbf{W}(\zeta) \odot \mathbf{\Gamma}_{\text{noise}})^{-1} = \begin{bmatrix} \mathbf{A} \odot \mathbf{W}_A & \mathbf{B} \odot \mathbf{W}_B \\ \mathbf{B}^\top \odot \mathbf{W}_B^\top & \mathbf{D} \odot \mathbf{W}_D \end{bmatrix}^{-1} = \begin{bmatrix} \tilde{\mathbf{A}} & \tilde{\mathbf{B}} \\ \tilde{\mathbf{B}}^\top & \tilde{\mathbf{D}} \end{bmatrix}^{-1} \\ &= \begin{bmatrix} (\tilde{\mathbf{A}} - \tilde{\mathbf{B}}\tilde{\mathbf{D}}^{-1}\tilde{\mathbf{B}}^\top)^{-1} & -(\tilde{\mathbf{A}} - \tilde{\mathbf{B}}\tilde{\mathbf{D}}^{-1}\tilde{\mathbf{B}}^\top)^{-1}\tilde{\mathbf{B}}\tilde{\mathbf{D}}^{-1} \\ -\tilde{\mathbf{D}}^{-1}\tilde{\mathbf{B}}^\top(\tilde{\mathbf{A}} - \tilde{\mathbf{B}}\tilde{\mathbf{D}}^{-1}\tilde{\mathbf{B}}^\top)^{-1} & \tilde{\mathbf{D}}^{-1} + \tilde{\mathbf{D}}^{-1}\tilde{\mathbf{B}}^\top(\tilde{\mathbf{A}} - \tilde{\mathbf{B}}\tilde{\mathbf{D}}^{-1}\tilde{\mathbf{B}}^\top)^{-1}\tilde{\mathbf{B}}\tilde{\mathbf{D}}^{-1} \end{bmatrix}. \end{aligned}$$

It follows from the first case (also from [Lemma 3.3](#)) that $\tilde{\mathbf{D}}^{-1} \rightarrow \mathbf{D}^{-1}$ for $\zeta \rightarrow \zeta^b$. Note that $(\tilde{\mathbf{A}} - \tilde{\mathbf{B}}\tilde{\mathbf{D}}^{-1}\tilde{\mathbf{B}}^\top)^{-1}$ appears in all blocks of $\mathbf{W}_\Gamma(\zeta)$. Thus, to achieve the desired result it suffices to show that $(\tilde{\mathbf{A}} - \tilde{\mathbf{B}}\tilde{\mathbf{D}}^{-1}\tilde{\mathbf{B}}^\top)^{-1} \rightarrow \mathbf{0}$ for $\zeta \rightarrow \zeta^b$, which implies $\mathbf{W}_\Gamma(\zeta) \rightarrow (\mathbf{\Gamma}_{\text{noise}} \odot \mathbf{W}(\zeta^b))^\dagger$ for $\zeta \rightarrow \zeta^b$. To this end, let us write $\zeta := (\zeta_A^\top, \zeta_B^\top)^\top$ and $\mathbf{s} := (\mathbf{s}_A^\top, \mathbf{s}_B^\top)^\top$. Thus, from both [\(A.1\)](#) and [\(A.7\)](#) it follows that

$$(A.8) \quad \begin{aligned} \mathbf{W}(\zeta) \odot \mathbf{\Gamma}_{\text{noise}} &= \begin{bmatrix} \mathbf{A} \odot \mathbf{W}_A & \mathbf{B} \odot \mathbf{W}_B \\ \mathbf{B}^\top \odot \mathbf{W}_B^\top & \mathbf{D} \odot \mathbf{W}_D \end{bmatrix} = \begin{bmatrix} \tilde{\mathbf{A}} & \tilde{\mathbf{B}} \\ \tilde{\mathbf{B}}^\top & \tilde{\mathbf{D}} \end{bmatrix} \\ &= \text{Diag}(\mathbf{s} \odot \mathbf{d}(\zeta)) + \text{Diag}(\zeta) \mathbf{\Gamma}_{\text{noise}} \text{Diag}(\zeta) \\ &= \begin{bmatrix} \text{Diag}(\mathbf{s}_A \odot \mathbf{d}(\zeta_A)) & \mathbf{0} \\ \mathbf{0} & \text{Diag}(\mathbf{s}_B \odot \mathbf{d}(\zeta_B)) \end{bmatrix} + \begin{bmatrix} \mathbf{A} \odot (\zeta_A \zeta_A^\top) & \mathbf{B} \odot (\zeta_A \zeta_B^\top) \\ \mathbf{B}^\top \odot (\zeta_B \zeta_A^\top) & \mathbf{D} \odot (\zeta_B \zeta_B^\top) \end{bmatrix}. \end{aligned}$$

Since for $\zeta \succ \mathbf{0}$, $\mathbf{\Gamma}_{\text{noise}} \succ \mathbf{0}$ it holds that $\text{Diag}(\zeta) \mathbf{\Gamma}_{\text{noise}} \text{Diag}(\zeta) \succ \mathbf{0}$, and given that $\mathbf{0} \preceq \zeta \preceq \mathbf{1}$, it follows from [\(A.8\)](#) that $\tilde{\mathbf{D}} \succeq \mathbf{D} \odot (\zeta_B \zeta_B^\top)$. Thus, it holds that

$$(A.9) \quad \begin{bmatrix} \mathbf{A} \odot (\zeta_A \zeta_A^\top) & \mathbf{B} \odot (\zeta_A \zeta_B^\top) \\ \mathbf{B}^\top \odot (\zeta_B \zeta_A^\top) & \tilde{\mathbf{D}} \end{bmatrix} = \begin{bmatrix} \mathbf{A} \odot (\zeta_A \zeta_A^\top) & \tilde{\mathbf{B}} \\ \mathbf{B}^\top & \tilde{\mathbf{D}} \end{bmatrix} \succeq \text{Diag}(\zeta) \mathbf{\Gamma}_{\text{noise}} \text{Diag}(\zeta) \succ \mathbf{0}.$$

From [\(A.9\)](#) and by utilizing the Shur complement, it follows that

$$(A.10) \quad \mathbf{A} \odot (\zeta_A \zeta_A^\top) - \tilde{\mathbf{B}}\tilde{\mathbf{D}}^{-1}\tilde{\mathbf{B}}^\top \succ \mathbf{0}.$$

By definition (see [\(A.8\)](#)) $\tilde{\mathbf{A}} = \text{Diag}(\mathbf{s}_A \odot \mathbf{d}(\zeta_A)) + \mathbf{A} \odot (\zeta_A \zeta_A^\top)$. Thus,

$$(A.11) \quad \tilde{\mathbf{A}} - \tilde{\mathbf{B}}\tilde{\mathbf{D}}^{-1}\tilde{\mathbf{B}}^\top = \text{Diag}(\mathbf{s}_A \odot \mathbf{d}(\zeta_A)) + \mathbf{A} \odot (\zeta_A \zeta_A^\top) - \tilde{\mathbf{B}}\tilde{\mathbf{D}}^{-1}\tilde{\mathbf{B}}^\top \stackrel{(A.10)}{\succ} \text{Diag}(\mathbf{s}_A \odot \mathbf{d}(\zeta_A)) \succ \mathbf{0},$$

which, by taking the inverse and applying the trace, implies $0 \leq \text{Tr}\left(\left(\tilde{\mathbf{A}} - \tilde{\mathbf{B}}\tilde{\mathbf{D}}^{-1}\tilde{\mathbf{B}}^\top\right)^{-1}\right) \leq \text{Tr}\left(\left(\text{Diag}(\mathbf{s}_A \odot \mathbf{d}(\zeta_A))\right)^{-1}\right)$ and $\text{Tr}\left(\left(\text{Diag}(\mathbf{s}_A \odot \mathbf{d}(\zeta_A))\right)^{-1}\right) \rightarrow 0$ for $\zeta \rightarrow \zeta^b$. That proves that $\left(\tilde{\mathbf{A}} - \tilde{\mathbf{B}}\tilde{\mathbf{D}}^{-1}\tilde{\mathbf{B}}^\top\right)^{-1} \rightarrow \mathbf{0}$ for $\zeta \rightarrow \zeta^b$. Note that although ζ whose limits are considered here always remain in $(0, 1)^{n_s}$, this is by no means restrictive, since the continuous mapping $\zeta \rightarrow (\mathbf{W}(\zeta) \odot \mathbf{\Gamma}_{\text{noise}})^\dagger$ with domain $(0, 1)^{n_s}$ uniquely extends to a continuous mapping with domain $[0, 1]^{n_s}$ being the closure of $(0, 1)^{n_s}$. \square

Proof of Lemma 3.6. It is enough to discuss the proof assuming the weighting function (3.12). For $\zeta \in (0, 1]^{n_s}$, the weighted precision matrix is invertible, and continuity of the gradient follows immediately. For $\zeta_i \rightarrow 0$, $\mathbf{W}_\Gamma(\zeta) \rightarrow \mathcal{O}(\omega_i^2)$ and $\eta_i \rightarrow \mathcal{O}(\omega_i^{-3})$. Thus, as $\zeta_i \rightarrow 0$, $\mathbf{W}_\Gamma(\zeta)\mathbf{e}_i\eta_i^\top\mathbf{W}_\Gamma(\zeta) \rightarrow \mathcal{O}(\omega_i^2\omega_i^{-3}\omega_i^2) = \mathcal{O}(\omega) \rightarrow 0$. This matches the definition of the derivative defined by (3.19) for $\omega_i = 0$. \square

Appendix B. A-Optimality Criterion and Gradient. Here we detail the derivation of the formulae of the gradient of the A-optimality criterion (3.16a) with respect to the relaxed design. Recall that for each $i = 1, 2, \dots, n_s$

$$(B.1) \quad \frac{\partial \Psi^{\text{GA}}(\zeta)}{\partial \zeta_i} = \text{Tr}\left(\frac{\partial \mathbf{P}\mathbf{\Gamma}_{\text{post}}(\zeta)\mathbf{P}^*}{\partial \zeta_i}\right) = -\text{Tr}\left(\mathbf{P}\mathbf{H}^{-1}(\zeta)\mathbf{F}^* \frac{\partial \mathbf{W}_\Gamma(\zeta)}{\partial \zeta_i} \mathbf{F}\mathbf{H}^{-1}(\zeta)\mathbf{P}^*\right).$$

B.1. Space correlations. In the case of temporally uncorrelated observations, by utilizing (3.20), then for each $i = 1, 2, \dots, n_s$ we have

$$(B.2) \quad \begin{aligned} \frac{\partial \Psi^{\text{GA}}(\zeta)}{\partial \zeta_i} &= \text{Tr}\left(\mathbf{P}\mathbf{H}^{-1}(\zeta)\mathbf{F}^*\mathbf{W}_\Gamma(\zeta) \bigoplus_{m=1}^{n_t} \left(\mathbf{e}_i((\mathbf{R}_m\mathbf{e}_i) \odot \eta_i)^\top + ((\mathbf{R}_m\mathbf{e}_i) \odot \eta_i)\mathbf{e}_i^\top\right) \mathbf{W}_\Gamma(\zeta)\mathbf{F}\mathbf{H}^{-1}(\zeta)\mathbf{P}^*\right) \\ &= 2 \text{Tr}\left(\mathbf{P}\mathbf{H}^{-1}(\zeta)\mathbf{F}^*\mathbf{W}_\Gamma(\zeta) \bigoplus_{m=1}^{n_t} \left((\mathbf{R}_m\mathbf{e}_i) \odot \eta_i\right) \mathbf{e}_i^\top\right) \mathbf{W}_\Gamma(\zeta)\mathbf{F}\mathbf{H}^{-1}(\zeta)\mathbf{P}^*, \end{aligned}$$

where the vector of weight derivatives η_i is given by (3.19). Since observation errors are assumed to be temporally uncorrelated (i.e., across observation time instances t_m), then, given (B.2), the gradient of the A-optimality criterion can be written in terms of cardinality vectors $\mathbf{e}_i \in \mathbb{R}^{n_s}$, as $\nabla_\zeta \Psi^{\text{GA}}(\zeta) = \sum_{i=1}^{n_s} \frac{\partial \Psi^{\text{GA}}(\zeta)}{\partial \zeta_i} \mathbf{e}_i$, resulting in the following form:

$$(B.3) \quad \begin{aligned} \nabla_\zeta \Psi^{\text{GA}}(\zeta) &= 2 \sum_{i=1}^{n_s} \mathbf{e}_i \text{Tr}\left(\mathbf{P}\mathbf{H}^{-1}(\zeta)\mathbf{F}^*\mathbf{W}_\Gamma(\zeta) \left(\bigoplus_{m=1}^{n_t} \left((\mathbf{R}_m\mathbf{e}_i) \odot \eta_i\right) \mathbf{e}_i^\top\right) \mathbf{W}_\Gamma(\zeta)\mathbf{F}\mathbf{H}^{-1}(\zeta)\mathbf{P}^*\right) \\ &= 2 \sum_{j=1}^{n_s} \mathbf{e}_i \text{Tr}\left(\mathbf{P}\mathbf{H}^{-1}(\zeta) \sum_{m=1}^{n_t} \mathbf{F}_{m,0}^* \mathbf{V}_m^\dagger(\zeta) \left((\mathbf{R}_m\mathbf{e}_i) \odot \eta_i\right) \mathbf{e}_i^\top \mathbf{V}_m^\dagger(\zeta) \mathbf{F}_{0,m} \mathbf{H}^{-1}(\zeta)\mathbf{P}^*\right) \\ &= 2 \sum_{m=1}^{n_t} \sum_{j=1}^{n_s} \mathbf{e}_i \text{Tr}\left(\mathbf{e}_i^\top \mathbf{V}_m^\dagger(\zeta) \mathbf{F}_{0,m} \mathbf{H}^{-1}(\zeta)\mathbf{P}^* \mathbf{P}\mathbf{H}^{-1}(\zeta)\mathbf{F}_{m,0}^* \mathbf{V}_m^\dagger(\zeta) \left((\mathbf{R}_m\mathbf{e}_i) \odot \eta_i\right) \mathbf{e}_i^\top\right) \\ &= 2 \sum_{j=1}^{n_s} \mathbf{e}_i \mathbf{e}_i^\top \sum_{m=1}^{n_t} \mathbf{V}_m^\dagger(\zeta) \mathbf{F}_{0,m} \mathbf{H}^{-1}(\zeta)\mathbf{P}^* \mathbf{P}\mathbf{H}^{-1}(\zeta)\mathbf{F}_{m,0}^* \mathbf{V}_m^\dagger(\zeta) \left((\mathbf{R}_m\mathbf{e}_i) \odot \eta_i\right) \mathbf{e}_i^\top, \end{aligned}$$

where as defined by (3.21),

$$(B.4) \quad \mathbf{W}_\Gamma(\zeta) = \bigoplus_{m=1}^{n_t} (\mathbf{V}_m^\dagger(\zeta)), \quad \mathbf{V}_m(\zeta) := \mathbf{R}_m \odot \left(\sum_{i,j=1}^{n_s} \varpi(\zeta_i, \zeta_j) \mathbf{e}_i \mathbf{e}_j^\top \right).$$

We used the circular property of matrix trace and the fact that, for a symmetric matrix \mathbf{A} and a vector \mathbf{y} with conformable shapes. Then $\mathbf{A} \odot (\mathbf{e}_i \mathbf{y}^\top) = \mathbf{e}_i ((\mathbf{e}_i^\top \mathbf{A}) \odot \mathbf{y}^\top) = \mathbf{e}_i ((\mathbf{A} \mathbf{e}_i) \odot \mathbf{y})^\top$. By utilizing the matrix of weights derivatives \mathbf{W}' defined by (3.23), we can refine (B.3) to

$$(B.5) \quad \nabla_\zeta \Psi^{\text{GA}}(\zeta) = 2 \sum_{m=1}^{n_t} \text{diag}(\mathbf{V}_m^\dagger(\zeta) \mathbf{F}_{0,m} \mathbf{H}^{-1}(\zeta) \mathbf{P}^* \mathbf{P} \mathbf{H}^{-1}(\zeta) \mathbf{F}_{m,0}^* \mathbf{V}_m^\dagger(\zeta) (\mathbf{R}_m \odot \mathbf{W}')) .$$

B.2. Spatiotemporal correlations. In the presence of spatiotemporal correlations, the derivative of the A-optimality criterion is obtained as follows. For each $i = 1, 2, \dots, n_s$

$$(B.6) \quad \begin{aligned} \frac{\partial \Psi^{\text{GA}}(\zeta)}{\partial \zeta_i} &= -\text{Tr} \left(\mathbf{P} \mathbf{H}^{-1}(\zeta) \mathbf{F}^* \frac{\partial \mathbf{W}_\Gamma(\zeta)}{\partial \zeta_i} \mathbf{F} \mathbf{H}^{-1}(\zeta) \mathbf{P}^* \right) \\ &= 2 \text{Tr} \left(\mathbf{P} \mathbf{H}^{-1}(\zeta) \mathbf{F}^* \mathbf{W}_\Gamma(\zeta) \left(\sum_{m=1}^{n_t} ((\mathbf{\Gamma}_{\text{noise}} \mathbf{e}_q) \odot \vartheta_{i,m}) \mathbf{e}_q^\top \right) \mathbf{W}_\Gamma(\zeta) \mathbf{F} \mathbf{H}^{-1}(\zeta) \mathbf{P}^* \right) \\ &= 2 \text{Tr} \left(\mathbf{e}_q^\top \mathbf{W}_\Gamma(\zeta) \mathbf{F} \mathbf{H}^{-1}(\zeta) \mathbf{P}^* \mathbf{P} \mathbf{H}^{-1}(\zeta) \mathbf{F}^* \mathbf{W}_\Gamma(\zeta) \sum_{m=1}^{n_t} ((\mathbf{\Gamma}_{\text{noise}} \mathbf{e}_q) \odot \vartheta_{i,m}) \right) \\ &= 2 \mathbf{e}_q^\top \mathbf{W}_\Gamma(\zeta) \mathbf{F} \mathbf{H}^{-1}(\zeta) \mathbf{P}^* \mathbf{P} \mathbf{H}^{-1}(\zeta) \mathbf{F}^* \mathbf{W}_\Gamma(\zeta) \sum_{m=1}^{n_t} ((\mathbf{\Gamma}_{\text{noise}} \mathbf{e}_q) \odot \vartheta_{i,m}), \end{aligned}$$

where $q = i + (m-1)n_s$ and the vector of weights derivatives $\vartheta_{i,m}$ is defined by (3.30). The gradient of the A-optimality criterion can be written as

$$(B.7) \quad \begin{aligned} \nabla_\zeta \Psi^{\text{GA}}(\zeta) &= 2 \sum_{i=1}^{n_s} \mathbf{e}_i \mathbf{e}_{i+(n-1)n_s}^\top \mathbf{W}_\Gamma(\zeta) \mathbf{F} \mathbf{H}^{-1}(\zeta) \mathbf{P}^* \mathbf{P} \mathbf{H}^{-1}(\zeta) \mathbf{F}^* \mathbf{W}_\Gamma(\zeta) \sum_{m=1}^{n_t} ((\mathbf{\Gamma}_{\text{noise}} \mathbf{e}_q) \odot \vartheta_{i,m}) \\ &= 2 \sum_{i=1}^{n_s} \sum_{m=1}^{n_t} \mathbf{e}_i \mathbf{e}_q^\top \mathbf{W}_\Gamma(\zeta) \mathbf{F} \mathbf{H}^{-1}(\zeta) \mathbf{P}^* \mathbf{P} \mathbf{H}^{-1}(\zeta) \mathbf{F}^* \mathbf{W}_\Gamma(\zeta) ((\mathbf{\Gamma}_{\text{noise}} \mathbf{e}_q) \odot \vartheta_{i,n}). \end{aligned}$$

B.3. A-optimal design with randomized trace estimator. A randomized approximation of the A-optimality criterion $\tilde{\Psi}^{\text{GA}}(\zeta) \approx \Psi^{\text{GA}}(\zeta)$, as defined by (3.34), takes the form

$$(B.8) \quad \begin{aligned} \tilde{\Psi}^{\text{GA}}(\zeta) &= \frac{1}{n_r} \sum_{r=1}^{n_r} \mathbf{z}_r^\top \boldsymbol{\Sigma}_{\text{post}}(\zeta) \mathbf{z}_r = \frac{1}{n_r} \sum_{r=1}^{n_r} \mathbf{z}_r^\top \mathbf{H}^{-1}(\zeta) \mathbf{z}_r \\ &= \frac{1}{n_r} \sum_{r=1}^{n_r} \mathbf{z}_r^\top \mathbf{P} (\mathbf{F}^* \mathbf{W}_\Gamma(\zeta) \mathbf{F} + \mathbf{\Gamma}_{\text{pr}}^{-1})^{-1} \mathbf{P}^* \mathbf{z}_r, \end{aligned}$$

where $\mathbf{z}_r \in \mathbb{R}^{N_{\text{goal}}}$ and $\mathbf{W}_\Gamma(\zeta)$ is given by (3.15). The gradient of this criterion follows directly as

$$(B.9) \quad \frac{\partial \tilde{\Psi}^{\text{GA}}(\zeta)}{\partial \zeta_i} = -\frac{1}{n_r} \sum_{r=1}^{n_r} \mathbf{z}_r^\top \mathbf{P} \mathbf{H}(\zeta)^{-1} \mathbf{F}^* \frac{\partial \mathbf{W}_\Gamma(\zeta)}{\partial \zeta_i} \mathbf{F} \mathbf{H}(\zeta)^{-1} \mathbf{P}^* \mathbf{z}_r.$$

This formula of the gradient can be refined given the exact formulation of the design matrix $\mathbf{W}(\zeta)$ and its derivative $\frac{\partial \mathbf{W}_\Gamma(\zeta)}{\partial \zeta_i}$, as discussed before. If we assume the observation errors are temporally uncorrelated, following the same procedure as in [Appendix B.1](#), then we have

$$(B.10) \quad \begin{aligned} \frac{\partial \tilde{\Psi}^{\text{GA}}(\zeta)}{\partial \zeta_i} &= \frac{1}{n_r} \sum_{r=1}^{n_r} \mathbf{z}_r^\top \mathbf{P} \mathbf{H}(\zeta)^{-1} \mathbf{F}^* \mathbf{W}_\Gamma(\zeta) \bigoplus_{m=1}^{n_t} \left(\mathbf{R}_m \odot \left(\mathbf{e}_i (\eta_i)^\top + \eta_i \mathbf{e}_i^\top \right) \right) \mathbf{W}_\Gamma(\zeta) \mathbf{F} \mathbf{H}(\zeta)^{-1} \mathbf{P}^* \mathbf{z}_r \\ &= \frac{2}{n_r} \sum_{r=1}^{n_r} \sum_{m=1}^{n_t} (\xi_{r,m}^*)^\top \mathbf{e}_i \left((\mathbf{R}_m \mathbf{e}_i) \odot \eta_i \right)^\top \xi_{r,m}, \end{aligned}$$

where η_i is given by [\(3.19\)](#), the vectors $\xi_{r,m}$ and $\xi_{r,m}^*$ are given by

$$(B.11) \quad \xi_{r,m} = \mathbf{V}_m^\dagger(\zeta) \mathbf{F}_{0,m} \mathbf{H}(\zeta)^{-1} \mathbf{P}^* \mathbf{z}_r; \quad (\xi_{r,m}^*)^\top = \mathbf{z}_r^\top \mathbf{P} \mathbf{H}(\zeta)^{-1} \mathbf{F}_{m,0}^* \mathbf{V}_m^\dagger(\zeta),$$

and $\mathbf{V}_m(\zeta)$ is given by [\(B.4\)](#). The full gradient, written in terms of its components, in this case is

$$(B.12) \quad \begin{aligned} \nabla_\zeta \tilde{\Psi}^{\text{GA}}(\zeta) &= \frac{2}{n_r} \sum_{i=1}^{n_s} \mathbf{e}_i \sum_{r=1}^{n_r} \sum_{m=1}^{n_t} (\xi_{r,m}^*)^\top \mathbf{e}_i \left((\mathbf{R}_m \mathbf{e}_i) \odot \eta_i \right)^\top \xi_{r,m} \\ &= \frac{2}{n_r} \sum_{r=1}^{n_r} \sum_{m=1}^{n_t} \xi_{r,m}^* \odot \left((\mathbf{R}_m \odot \mathbf{W}') \xi_{r,m} \right), \end{aligned}$$

with \mathbf{W}' defined by [\(3.23\)](#). In the presence of spatiotemporal correlations, the gradient is found as follows:

$$(B.13) \quad \begin{aligned} \frac{\partial \tilde{\Psi}^{\text{GA}}(\zeta)}{\partial \zeta_i} &= \frac{1}{n_r} \sum_{r=1}^{n_r} \mathbf{z}_r^\top \mathbf{P} \mathbf{H}^{-1}(\zeta) \mathbf{F}^* \mathbf{W}_\Gamma(\zeta) \left(\mathbf{\Gamma}_{\text{noise}} \odot \sum_{m=1}^{n_t} \left(\mathbf{e}_q \vartheta_{i,m}^\top + \vartheta_{i,m} \mathbf{e}_q^\top \right) \right) \mathbf{W}_\Gamma(\zeta) \mathbf{F} \mathbf{H}^{-1}(\zeta) \mathbf{P}^* \mathbf{z}_r \\ &= \frac{2}{n_r} \sum_{r=1}^{n_r} \mathbf{z}_r^\top \mathbf{P} \mathbf{H}^{-1}(\zeta) \mathbf{F}^* \mathbf{W}_\Gamma(\zeta) \left(\mathbf{\Gamma}_{\text{noise}} \odot \sum_{m=1}^{n_t} \left(\mathbf{e}_q \vartheta_{i,m}^\top \right) \right) \mathbf{W}_\Gamma(\zeta) \mathbf{F} \mathbf{H}^{-1}(\zeta) \mathbf{P}^* \mathbf{z}_r \\ &= \frac{2}{n_r} \sum_{r=1}^{n_r} \sum_{m=1}^{n_t} \psi_r^* \mathbf{e}_q \left((\mathbf{\Gamma}_{\text{noise}} \mathbf{e}_q) \odot \vartheta_{i,m} \right)^\top \psi_r, \end{aligned}$$

where $q = i + (m-1)n_s$, $\psi_r = \mathbf{W}_\Gamma(\zeta) \mathbf{F} \mathbf{H}(\zeta)^{-1} \mathbf{P}^* \mathbf{z}_r$, and $\psi_r^* = \mathbf{z}_r^\top \mathbf{P} \mathbf{H}(\zeta)^{-1} \mathbf{F}^* \mathbf{W}_\Gamma(\zeta)$. The full gradient follows as

$$(B.14) \quad \begin{aligned} \nabla_\zeta \tilde{\Psi}^{\text{GA}}(\zeta) &= \frac{2}{n_r} \sum_{i=1}^{n_s} \mathbf{e}_i \sum_{r=1}^{n_r} \sum_{m=1}^{n_t} \psi_r^* \mathbf{e}_{i+(m-1)n_s} \left((\mathbf{\Gamma}_{\text{noise}} \mathbf{e}_{i+(m-1)n_s}) \odot \vartheta_{i,m} \right)^\top \psi_r \\ &= \frac{2}{n_r} \sum_{r=1}^{n_r} \sum_{i=1}^{n_s} \sum_{m=1}^{n_t} \mathbf{e}_i \psi_r^* \mathbf{e}_{i+(m-1)n_s} \left((\mathbf{\Gamma}_{\text{noise}} \mathbf{e}_{i+(m-1)n_s}) \odot \vartheta_{i,m} \right)^\top \psi_r. \end{aligned}$$

Appendix C. D-Optimality Criterion and Gradient. When the D-optimality is set as the OED criterion, that is, by defining the optimal design using [\(3.16b\)](#), the derivative of the

optimization objective w.r.t the design variables ζ_i , $i = 1, 2, \dots, n_s$, is

$$(C.1) \quad \begin{aligned} \frac{\partial \Psi^{\text{GD}}(\zeta)}{\partial \zeta_i} &= \text{Tr} \left(\boldsymbol{\Sigma}_{\text{post}}^{-1}(\zeta) \frac{\partial \mathbf{P} \boldsymbol{\Gamma}_{\text{post}}(\zeta) \mathbf{P}^*}{\partial \zeta_i} \right) \\ &= -\text{Tr} \left(\boldsymbol{\Sigma}_{\text{post}}^{-1}(\zeta) \mathbf{P} \mathbf{H}^{-1}(\zeta) \mathbf{F}^* \frac{\partial \mathbf{W}_{\Gamma}(\zeta)}{\partial \zeta_i} \mathbf{F} \mathbf{H}^{-1}(\zeta) \mathbf{P}^* \right). \end{aligned}$$

C.1. Space correlations. For the sake of derivation, we define the Cholesky factorization of the prediction covariance as $\boldsymbol{\Sigma}_{\text{post}}(\zeta) = \boldsymbol{\Sigma}_{\text{post}}^{1/2} \boldsymbol{\Sigma}_{\text{post}}^{T/2}$, with $\boldsymbol{\Sigma}_{\text{post}}^{1/2}$ being the lower triangular factor. Moreover, the dimensionality of the prediction QoI is generally small, and such factorization if needed is inexpensive. Then, $\boldsymbol{\Sigma}_{\text{post}}^{-1}(\zeta) = \boldsymbol{\Sigma}_{\text{post}}^{-1/2} \boldsymbol{\Sigma}_{\text{post}}^{-T/2}$ with $\boldsymbol{\Sigma}_{\text{post}}^{-1/2} = \left(\boldsymbol{\Sigma}_{\text{post}}^{1/2} \right)^{-1}$. The gradient of the D-optimality criterion follows as

$$(C.2) \quad \begin{aligned} \nabla_{\zeta} \Psi^{\text{GD}}(\zeta) &= - \sum_{i=1}^{n_s} \mathbf{e}_i \text{Tr} \left(\boldsymbol{\Sigma}_{\text{post}}^{-1}(\zeta) \mathbf{P} \mathbf{H}^{-1}(\zeta) \mathbf{F}^* \frac{\partial \mathbf{W}_{\Gamma}(\zeta)}{\partial \zeta_i} \mathbf{F} \mathbf{H}^{-1}(\zeta) \mathbf{P}^* \right) \\ &= \sum_{i=1}^{n_s} \mathbf{e}_i \text{Tr} \left(\boldsymbol{\Sigma}_{\text{post}}^{-\frac{T}{2}} \mathbf{P} \mathbf{H}^{-1}(\zeta) \mathbf{F}^* \mathbf{W}_{\Gamma}(\zeta) \bigoplus_{m=1}^{n_t} (\mathbf{R}_m \odot (\mathbf{e}_i (\eta_i)^{\text{T}} + \eta_i \mathbf{e}_i^{\text{T}})) \mathbf{W}_{\Gamma}(\zeta) \mathbf{F} \mathbf{H}^{-1}(\zeta) \mathbf{P}^* \boldsymbol{\Sigma}_{\text{post}}^{-\frac{1}{2}} \right) \\ &= 2 \sum_{i=1}^{n_s} \mathbf{e}_i \text{Tr} \left(\boldsymbol{\Sigma}_{\text{post}}^{-\frac{T}{2}} \mathbf{P} \mathbf{H}^{-1}(\zeta) \mathbf{F}^* \mathbf{W}_{\Gamma}(\zeta) \bigoplus_{m=1}^{n_t} (\mathbf{R}_m \odot (\eta_i \mathbf{e}_i^{\text{T}})) \mathbf{W}_{\Gamma}(\zeta) \mathbf{F} \mathbf{H}^{-1}(\zeta) \mathbf{P}^* \boldsymbol{\Sigma}_{\text{post}}^{-\frac{1}{2}} \right) \\ &= 2 \sum_{i=1}^{n_s} \mathbf{e}_i \sum_{m=1}^{n_t} \text{Tr} \left(\boldsymbol{\Sigma}_{\text{post}}^{-\frac{T}{2}} \mathbf{P} \mathbf{H}^{-1}(\zeta) \mathbf{F}^*_{m,0} \mathbf{V}_m^{\dagger}(\zeta) ((\mathbf{R}_m \mathbf{e}_i) \odot \eta_i) \mathbf{e}_i^{\text{T}} \mathbf{V}_m^{\dagger}(\zeta) \mathbf{F}_{0,m} \mathbf{H}^{-1}(\zeta) \mathbf{P}^* \boldsymbol{\Sigma}_{\text{post}}^{-\frac{1}{2}} \right) \\ &= 2 \sum_{i=1}^{n_s} \mathbf{e}_i \mathbf{e}_i^{\text{T}} \sum_{m=1}^{n_t} \mathbf{V}_m^{\dagger}(\zeta) \mathbf{F}_{0,m} \mathbf{H}^{-1}(\zeta) \mathbf{P}^* \boldsymbol{\Sigma}_{\text{post}}^{-1}(\zeta) \mathbf{P} \mathbf{H}^{-1}(\zeta) \mathbf{F}^*_{m,0} \mathbf{V}_m^{\dagger}(\zeta) ((\mathbf{R}_m \mathbf{e}_i) \odot \eta_i) \\ &= 2 \sum_{m=1}^{n_t} \text{diag} \left(\mathbf{V}_m^{\dagger}(\zeta) \mathbf{F}_{0,m} \mathbf{H}^{-1}(\zeta) \mathbf{P}^* \boldsymbol{\Sigma}_{\text{post}}^{-1}(\zeta) \mathbf{P} \mathbf{H}^{-1}(\zeta) \mathbf{F}^*_{m,0} \mathbf{V}_m^{\dagger}(\zeta) (\mathbf{R}_m \odot \mathbf{W}') \right), \end{aligned}$$

where we used the circular property of the matrix trace and the fact that the trace is invariant under matrix transposition and $\mathbf{V}_m^{\dagger}(\zeta)$ is given by (B.4).

C.2. Spatiotemporal correlations. The gradient of the D-optimality criterion in this case is (C.3)

$$\begin{aligned}
\nabla_{\zeta} \Psi^{\text{GD}}(\zeta) &= - \sum_{i=1}^{n_s} \mathbf{e}_i \text{Tr} \left(\Sigma_{\text{post}}^{-1} \mathbf{P} \mathbf{H}^{-1}(\zeta) \mathbf{F}^* \frac{\partial \mathbf{W}_{\Gamma}(\zeta)}{\partial \zeta_i} \mathbf{F} \mathbf{H}^{-1}(\zeta) \mathbf{P}^* \right) \\
&= \sum_{i=1}^{n_s} \mathbf{e}_i \text{Tr} \left(\Sigma_{\text{post}}^{-1} \mathbf{P} \mathbf{H}^{-1}(\zeta) \mathbf{F}^* \mathbf{W}_{\Gamma}(\zeta) \left(\Gamma_{\text{noise}} \odot \sum_{m=1}^{n_t} (\mathbf{e}_q \vartheta_{i,m}^{\top} + \vartheta_{i,m} \mathbf{e}_q^{\top}) \right) \mathbf{W}_{\Gamma}(\zeta) \mathbf{F} \mathbf{H}^{-1}(\zeta) \mathbf{P}^* \right) \\
&= 2 \sum_{i=1}^{n_s} \mathbf{e}_i \text{Tr} \left(\Sigma_{\text{post}}^{-1} \mathbf{P} \mathbf{H}^{-1}(\zeta) \mathbf{F}^* \mathbf{W}_{\Gamma}(\zeta) \left(\Gamma_{\text{noise}} \odot \sum_{m=1}^{n_t} (\mathbf{e}_q \vartheta_{i,m}^{\top}) \right) \mathbf{W}_{\Gamma}(\zeta) \mathbf{F} \mathbf{H}^{-1}(\zeta) \mathbf{P}^* \right) \\
&= 2 \sum_{i=1}^{n_s} \mathbf{e}_i \sum_{m=1}^{n_t} \text{Tr} \left(\Sigma_{\text{post}}^{-1} \mathbf{P} \mathbf{H}^{-1}(\zeta) \mathbf{F}^* \mathbf{W}_{\Gamma}(\zeta) (\Gamma_{\text{noise}} \odot (\mathbf{e}_q \vartheta_{i,m}^{\top})) \mathbf{W}_{\Gamma}(\zeta) \mathbf{F} \mathbf{H}^{-1}(\zeta) \mathbf{P}^* \right) \\
&= 2 \sum_{i=1}^{n_s} \mathbf{e}_i \sum_{m=1}^{n_t} \text{Tr} \left(\Sigma_{\text{post}}^{-1} \mathbf{P} \mathbf{H}^{-1}(\zeta) \mathbf{F}^* \mathbf{W}_{\Gamma}(\zeta) \mathbf{e}_q (\Gamma_{\text{noise}} \mathbf{e}_q \odot \vartheta_{i,m})^{\top} \mathbf{W}_{\Gamma}(\zeta) \mathbf{F} \mathbf{H}^{-1}(\zeta) \mathbf{P}^* \right) \\
&= 2 \sum_{i=1}^{n_s} \sum_{m=1}^{n_t} \mathbf{e}_i (\Gamma_{\text{noise}} \mathbf{e}_q \odot \vartheta_{i,m})^{\top} \mathbf{W}_{\Gamma}(\zeta) \mathbf{F} \mathbf{H}^{-1}(\zeta) \mathbf{P}^* \Sigma_{\text{post}}^{-1} \mathbf{P} \mathbf{H}^{-1}(\zeta) \mathbf{F}^* \mathbf{W}_{\Gamma}(\zeta) \mathbf{e}_q,
\end{aligned}$$

where $\mathbf{e}_q \equiv \mathbf{e}_{i+(m-1)n_s} \in \mathbb{R}^{N_{\text{obs}}}$; $i = 1, 2, \dots, n_s$, $m = 1, 2, \dots, n_t$.

Appendix D. Additional Numerical Results. In this section we give additional empirical results to complement the work presented in Section 4.

D.1. Reduced-order approximation of Hessian. Here we give more details about the approach used to develop a reduced-order approximation of the Hessian operator in the Bayesian inverse problem. This complements the discussion in Section 4

Repeated evaluation of Hessian matrix-vector products is computationally demanding. We use the two-pass algorithm described in [45] to generate a randomized reduced-order approximation of the Hessian \mathbf{H} . The number of eigenvalues is set to 80, and the oversampling parameter is $p = 20$. Figure 13 shows the leading $\lambda = 80$ eigenvalues, with approximation error. Fast decay in eigenvalues,

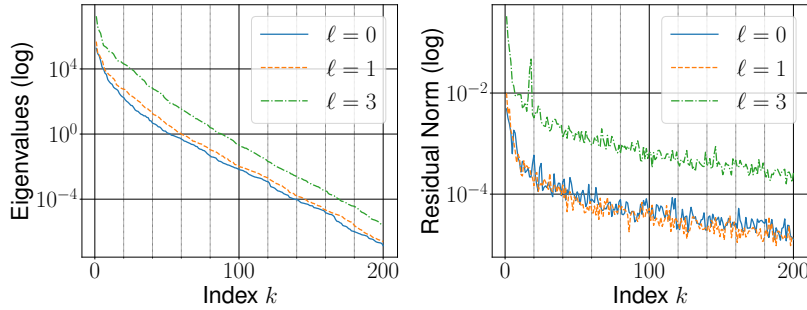


FIG. 13. Leading eigenvalues, on a logarithmic scale, of the Hessian \mathbf{H} obtained by the two-pass algorithm [45], along with the residual norms. Results are obtained with all sensors activated, i.e., $\zeta = \mathbf{1}$.

with over 99% of the variance explained by the leading 80 eigenvalues in all three cases, supports the accuracy of the reduced-order approximation of the Hessian.

D.2. Randomized estimator of the A-optimality criterion. In the numerical experiments in Section 4 we used the Hutchinson randomized trace estimator to approximate the A-optimality criterion, which enabled us to carry out several comparative experiments efficiently, and we set the sample size to $n_r = 25$, which we believed would achieve a highly accurate estimate of the optimality criterion. To test the validity of this assertion, in our settings we compared the exact value of the posterior covariance trace with the randomized approximation. Results indicating the accuracy of the posterior trace approximation by randomization are shown in Figure 14. The value of the Hutchinson randomized trace estimator was evaluated for the three experimental setups discussed in this section. In each case, the trace estimate of the posterior covariance matrix trace was evaluated by using several choices of the sample size n_r . For each experimental setting and for each choice of the sample size, the trace approximation was carried out 100 times, each with a new sample. The red stars show the true value of the posterior covariance trace in each case. These results show that even using a sample of size $n_r = 1$ generated from Rademacher distribution, we obtain a good approximation of the trace of the posterior covariance matrix, albeit exhibiting high variability around the true value. A much better estimate of the true value can be obtained by increasing the sample size n_r . Thus, in our experiments we followed this approach to approximate the A-optimality criterion, which enabled us to carry out several comparative experiments efficiently, and we set the sample size to $n_r = 25$.

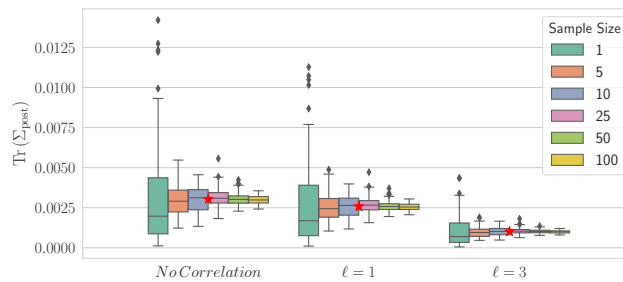


FIG. 14. Results showing accuracy of posterior trace approximation by randomization using the Hutchinson trace estimator. Box plots are shown for the three cases studied in this section. The first case considers the setup with no observation correlations, and the other cases correspond to the experiments where observation correlations are synthesized with length-scale ℓ set to 1 and 3, respectively. The true value of the posterior covariance trace $\text{Tr}(\Sigma_{\text{post}})$ is plotted as a red star for each case. In each case the randomized trace is calculated by using various choices of the sample size n_r , where the random vectors are sampled from Rademacher distribution. The trace approximation is carried out 100 times for each choice of the sample size and for each case to generate the boxplots.

Acknowledgments. This work was partially supported by the U.S. Department of Energy, Office of Science, Advanced Scientific Computing Research Program under contract DE-AC02-06CH11357 and Laboratory Directed Research and Development (LDRD) funding from Argonne National Laboratory. We thank three anonymous referees and the associate editor for their detailed and insightful comments that helped us improve our manuscript.

REFERENCES

- [1] A. ALEXANDERIAN, *Optimal experimental design for infinite-dimensional Bayesian inverse problems governed by PDEs: A review*, Inverse Problems, 37 (2021), p. 043001.

- [2] A. ALEXANDERIAN, P. J. GLOOR, O. GHATTAS, ET AL., *On Bayesian A-and D-optimal experimental designs in infinite dimensions*, Bayesian Analysis, 11 (2016), pp. 671–695.
- [3] A. ALEXANDERIAN, N. PETRA, G. STADLER, AND O. GHATTAS, *A-optimal design of experiments for infinite-dimensional Bayesian linear inverse problems with regularized ℓ_0 -sparsification*, SIAM Journal on Scientific Computing, 36 (2014), pp. A2122–A2148, <https://doi.org/10.1137/130933381>.
- [4] A. ALEXANDERIAN, N. PETRA, G. STADLER, AND O. GHATTAS, *A fast and scalable method for A-optimal design of experiments for infinite-dimensional Bayesian nonlinear inverse problems*, SIAM Journal on Scientific Computing, 38 (2016), pp. A243–A272, <https://doi.org/10.1137/140992564>.
- [5] A. ALEXANDERIAN AND A. K. SAIBABA, *Efficient d-optimal design of experiments for infinite-dimensional Bayesian linear inverse problems*, SIAM Journal on Scientific Computing, 40 (2018), pp. A2956–A2985.
- [6] A. ATTIA, A. ALEXANDERIAN, AND A. K. SAIBABA, *Goal-oriented optimal design of experiments for large-scale Bayesian linear inverse problems*, Inverse Problems, 34 (2018), p. 095009.
- [7] A. ATTIA AND E. CONSTANTINESCU, *An optimal experimental design framework for adaptive inflation and covariance localization for ensemble filters*, arXiv preprint arXiv:1806.10655, (2018).
- [8] A. ATTIA, S. LEYFFER, AND T. S. MUNSON, *Stochastic learning approach for binary optimization: Application to Bayesian optimal design of experiments*, SIAM Journal on Scientific Computing, 44 (2022), pp. B395–B427.
- [9] A. ATTIA AND A. SANDU, *A Hybrid Monte Carlo sampling filter for non-Gaussian data assimilation*, AIMS Geosciences, 1 (2015), pp. 41–78, <https://doi.org/http://dx.doi.org/10.3934/geosci.2015.1.41>, <http://www.aimspress.com/geosciences/article/574.html>.
- [10] A. ATTIA, R. ȘTEFĂNESCU, AND A. SANDU, *The reduced-order Hybrid Monte Carlo sampling smoother*, International Journal for Numerical Methods in Fluids, 83 (2017), pp. 28–51, <https://doi.org/10.1002/flid.4255>.
- [11] H. AVRON AND S. TOLEDO, *Randomized algorithms for estimating the trace of an implicit symmetric positive semi-definite matrix*, Journal of the ACM (JACM), 58 (2011), pp. 1–34.
- [12] R. BANNISTER, *A review of operational methods of variational and ensemble-variational data assimilation*, Quarterly Journal of the Royal Meteorological Society, 143 (2017), pp. 607–633.
- [13] T. BUI-THANH, O. GHATTAS, J. MARTIN, AND G. STADLER, *A computational framework for infinite-dimensional Bayesian inverse problems part i: The linearized case, with application to global seismic inversion*, SIAM Journal on Scientific Computing, 35 (2013), pp. A2494–A2523.
- [14] T. BUI-THANH, O. GHATTAS, J. MARTIN, AND G. STADLER, *A computational framework for infinite-dimensional Bayesian inverse problems Part I: The linearized case, with application to global seismic inversion*, SIAM Journal on Scientific Computing, 35 (2013), pp. A2494–A2523, <https://doi.org/10.1137/12089586X>.
- [15] R. H. BYRD, P. LU, J. NOCEDAL, AND C. ZHU, *A limited memory algorithm for bound constrained optimization*, SIAM Journal on Scientific Computing, 16 (1995), pp. 1190–1208.
- [16] K. CHALONER AND I. VERDINELLI, *Bayesian experimental design: A review*, Statistical Science, 10 (1995), pp. 273–304.
- [17] N. CRESSIE AND C. K. WIKLE, *Statistics for spatio-temporal data*, John Wiley & Sons, 2015.
- [18] R. DALEY, *Atmospheric data analysis*, Cambridge University Press, 1991.
- [19] H. DETTE, A. PEPELYSHEV, A. ZHIGLJAVSKY, ET AL., *Optimal design for linear models with correlated observations*, The Annals of Statistics, 41 (2013), pp. 143–176.
- [20] V. FEDOROV AND J. LEE, *Design of experiments in statistics*, in Handbook of semidefinite programming, R. S. H. Wolkowicz and L. Vandenberghe, eds., vol. 27 of Internat. Ser. Oper. Res. Management Sci., Kluwer Acad. Publ., Boston, MA, 2000, pp. 511–532.
- [21] V. V. FEDOROV, *Theory of optimal experiments*, Elsevier, 2013.
- [22] G. GASPARI AND S. E. COHN, *Construction of correlation functions in two and three dimensions*, Quarterly Journal of the Royal Meteorological Society, 125 (1999), pp. 723–757.
- [23] E. HABER, L. HORESH, AND L. TENORIO, *Numerical methods for experimental design of large-scale linear ill-posed inverse problems*, Inverse Problems, 24 (2008), pp. 125–137.
- [24] E. HABER, L. HORESH, AND L. TENORIO, *Numerical methods for the design of large-scale nonlinear discrete ill-posed inverse problems*, Inverse Problems, 26 (2010), p. 025002.
- [25] E. HABER, Z. MAGNANT, C. LUCERO, AND L. TENORIO, *Numerical methods for A-optimal designs with a sparsity constraint for ill-posed inverse problems*, Computational Optimization and Applications, (2012), pp. 1–22.
- [26] T. M. HAMILL AND J. S. WHITAKER, *Distance-dependent filtering of background error covariance estimates in an ensemble Kalman filter*, Monthly Weather Review, 129 (2001), pp. 2776–2790.
- [27] E. HERMAN, A. ALEXANDERIAN, AND A. K. SAIBABA, *Randomization and reweighted ℓ_1 -minimization for A-optimal design of linear inverse problems*, arXiv preprint arXiv:1906.03791, (2019).
- [28] R. A. HORN, *The Hadamard product*, vol. 40, American Mathematical Society, Proceedings of Symposia in Applied Mathematics, 1990, pp. 87–169.
- [29] X. HUAN AND Y. M. MARZOUK, *Simulation-based optimal Bayesian experimental design for nonlinear systems*,

- Journal of Computational Physics, 232 (2013), pp. 288–317, <https://doi.org/http://dx.doi.org/10.1016/j.jcp.2012.08.013>.
- [30] K. KOVAL, A. ALEXANDERIAN, AND G. STADLER, *Optimal experimental design under irreducible uncertainty for linear inverse problems governed by pdes*, Inverse Problems, (2020).
 - [31] S. LIU, S. P. CHEPURI, M. FARDAD, E. MAŞAZADE, G. LEUS, AND P. K. VARSHNEY, *Sensor selection for estimation with correlated measurement noise*, IEEE Transactions on Signal Processing, 64 (2016), pp. 3509–3522.
 - [32] K. LÖWNER, *Über monotone matrixfunktionen*, Mathematische Zeitschrift, 38 (1934), pp. 177–216.
 - [33] A. MOOSAVI, A. ATTIA, AND A. SANDU, *Tuning covariance localization using machine learning*, in International Conference on Computational Science, Springer, 2019, pp. 199–212.
 - [34] W. G. MÜLLER, *Collecting spatial data: Optimum design of experiments for random fields*, Springer Science & Business Media, 2007.
 - [35] W. NÄTHER, *Effective observation of random fields*, vol. 72, Teubner, 1985.
 - [36] I. M. NAVON, *Data assimilation for numerical weather prediction: a review*, in Data assimilation for atmospheric, oceanic and hydrologic applications, Springer, 2009, pp. 21–65.
 - [37] A. PAZMAN, *A convergence theorem in the theory of D-optimum experimental designs*, The Annals of Statistics, (1974), pp. 216–218.
 - [38] A. PÁZMAN, *Foundations of optimum experimental design*, D. Reidel Publishing Co., 1986.
 - [39] N. PETRA AND G. STADLER, *Model variational inverse problems governed by partial differential equations*, Tech. Report 11-05, The Institute for Computational Engineering and Sciences, The University of Texas at Austin, 2011.
 - [40] J. PILZ AND J. PILZ, *Bayesian estimation and experimental design in linear regression models*, vol. 212, Wiley New York, 1991.
 - [41] L. PRONZATO AND A. PÁZMAN, *Design of experiments in nonlinear models*, Lecture notes in statistics, 212 (2013), p. 1.
 - [42] F. PUKELSHEIM, *Optimal design of experiments*, SIAM, 2006.
 - [43] S. SAGER, *Sampling decisions in optimum experimental design in the light of Pontryagin’s maximum principle*, SIAM Journal on Control and Optimization, 51 (2013), pp. 3181–3207.
 - [44] A. K. SAIBABA, J. LEE, AND P. K. KITANIDIS, *Randomized algorithms for generalized Hermitian eigenvalue problems with application to computing Karhunen–Loève expansion*, Numerical Linear Algebra with Applications, 23 (2016), pp. 314–339.
 - [45] A. K. SAIBABA, J. LEE, AND P. K. KITANIDIS, *Randomized algorithms for generalized Hermitian eigenvalue problems with application to computing Karhunen–Loève expansion*, Numerical Linear Algebra with Applications, 23 (2016), pp. 314–339.
 - [46] SCIPY, *Python implementation of the L-BFGS-B algorithm*. https://docs.scipy.org/doc/scipy-0.14.0/reference/generated/scipy.optimize.fmin_l_bfgs_b.html, 2017.
 - [47] D. UCIŃSKI, *Optimal sensor location for parameter estimation of distributed processes*, International Journal of Control, 73 (2000), pp. 1235–1248.
 - [48] D. UCIŃSKI, *D-optimal sensor selection in the presence of correlated measurement noise*, Measurement, 164 (2020), p. 107873.
 - [49] D. UCIŃSKI AND A. C. ATKINSON, *Experimental design for time-dependent models with correlated observations*, Studies in Nonlinear Dynamics & Econometrics, 8 (2004).
 - [50] U. VILLA, N. PETRA, AND O. GHATTAS, *hIPPYlib: An extensible software framework for large-scale deterministic and linearized Bayesian inversion*, (2016). <http://hippylib.github.io>.
 - [51] J. S. WHITAKER AND T. M. HAMILL, *Ensemble data assimilation without perturbed observations*, Monthly Weather Review, 130 (2002), pp. 1913–1924.
 - [52] H. P. WYNN, *The sequential generation of D-optimum experimental designs*, The Annals of Mathematical Statistics, 41 (1970), pp. 1655–1664.
 - [53] J. YU, V. M. ZAVALA, AND M. ANITESCU, *A scalable design of experiments framework for optimal sensor placement*, Journal of Process Control, (2017).

The submitted manuscript has been created by UChicago Argonne, LLC, Operator of Argonne National Laboratory (“Argonne”). Argonne, a U.S. Department of Energy Office of Science laboratory, is operated under Contract No. DE-AC02-06CH11357. The U.S. Government retains for itself, and others acting on its behalf, a paid-up nonexclusive, irrevocable worldwide license in said article to reproduce, prepare derivative works, distribute copies to the public, and perform publicly and display publicly, by or on behalf of the Government. The Department of Energy will provide public access to these results of federally sponsored research in accordance with the DOE Public Access Plan. <http://energy.gov/downloads/doe-public-access-plan>.